# Supporting Information for "The 2020 $M_w$ 6.8 Elazığ (Turkey) earthquake reveals rupture behavior of the East Anatolian Fault"

Léa Pousse-Beltran[1], Edwin Nissen[1], Eric A. Bergman[2], Musavver Didem

Cambaz[3], Élyse Gaudreau[1], Ezgi Karasözen[4], and Fengzhou Tan[1]

[1]School of Earth and Ocean Sciences, University of Victoria, Victoria BC, Canada

[2]Global Seismological Services, Golden CO, USA

[3]Kandilli Observatory and Earthquake Research Institute, Boğaziçi University, İstanbul, Turkey

[4]Alaska Earthquake Center, University of Alaska Fairbanks, Fairbanks AK, USA

## Contents of this file

1. Text S1.

2. Figures S1 to S10.

3. Tables S1 to S11.

### Text S1: elastic and velocity model details

We have endeavoured to use consistent velocity and elastic models throughout this study. The best constraints on regional crustal velocities are provided by the multiple-event relocations. We settled upon the crustal velocities shown in Figure S1; below the Moho, we used velocities from the *ak135* 1-D Earth model (Kennett et al., 1995), which

————

from our previous experience are appropriate for the Middle East. We used the same velocities for modeling regional waveforms. For the InSAR modeling, we used a simplified elastic half-space with Lamé parameters $\mu = \lambda = 3.2 \times 10^{10}$ Pa. For the back projection, we calculated theoretical travel times from a grid of nodes across the source region to each station using the Kennett and Engdahl (1991) 1-D Earth model.

**References**

Duman, T. Y., & Emre, O. (2013). The East Anatolian Fault: geometry, segmentation and jog characteristics. In A. H. F. Robertson, O. Parlak, & U. C. Ünlügenç (Eds.), *Geological Development of Anatolia and the Easternmost Mediterranean Region* (Vol. 372, pp. 495–529). Geol. Soc. London Spec. Publ..

Kennett, B. L. N., & Engdahl, E. R. (1991, May). Traveltimes for Global Earthquake Location and Phase Identification. *Geophys. J. Int.*, *105*, 429–465.

Kennett, B. L. N., Engdahl, E. R., & Buland, R. (1995, July). Constraints on seismic velocities in the Earth from traveltimes. *Geophys. J. Int.*, *122*, 108–124.

Sokos, E., & Zahradník, J. (2013). Evaluating Centroid-Moment-Tensor Uncertainty in the New Version of ISOLA Software. *Seismol. Res. Lett.*, *84*(4), 656–665.

Sokos, E. N., & Zahradník, J. (2008). ISOLA a Fortran code and a Matlab GUI to perform multiple-point source inversion of seismic data. *Computers & Geosciences*, *34*, 967–977.
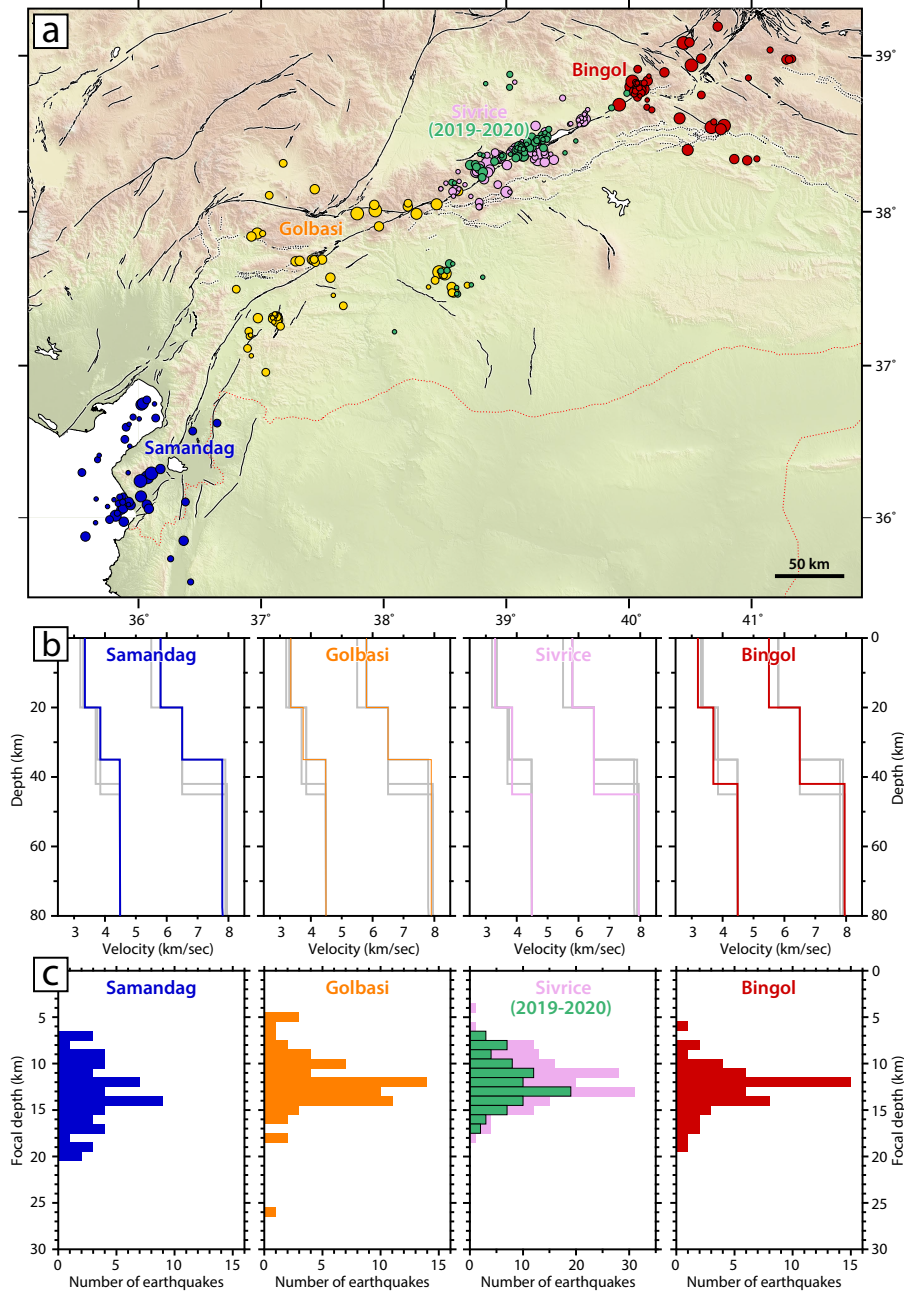
**Figure S1.** (a) Relocated seismicity along the East Anatolian Fault colored according to the relocation cluster. The Sivrice cluster is split in two, one focused on background seismicity and the other on 2019–2020 events. Earthquakes are scaled by magnitude as in Figure 1c of the main paper. (b) Panels showing crustal and upper mantle $P$ wave (left) and $S$ wave (right) velocities used in each cluster. Velocities used in other clusters are shown in gray. (c) Relocated focal depth distribution of each cluster.

March 25, 2020, 9:12pm
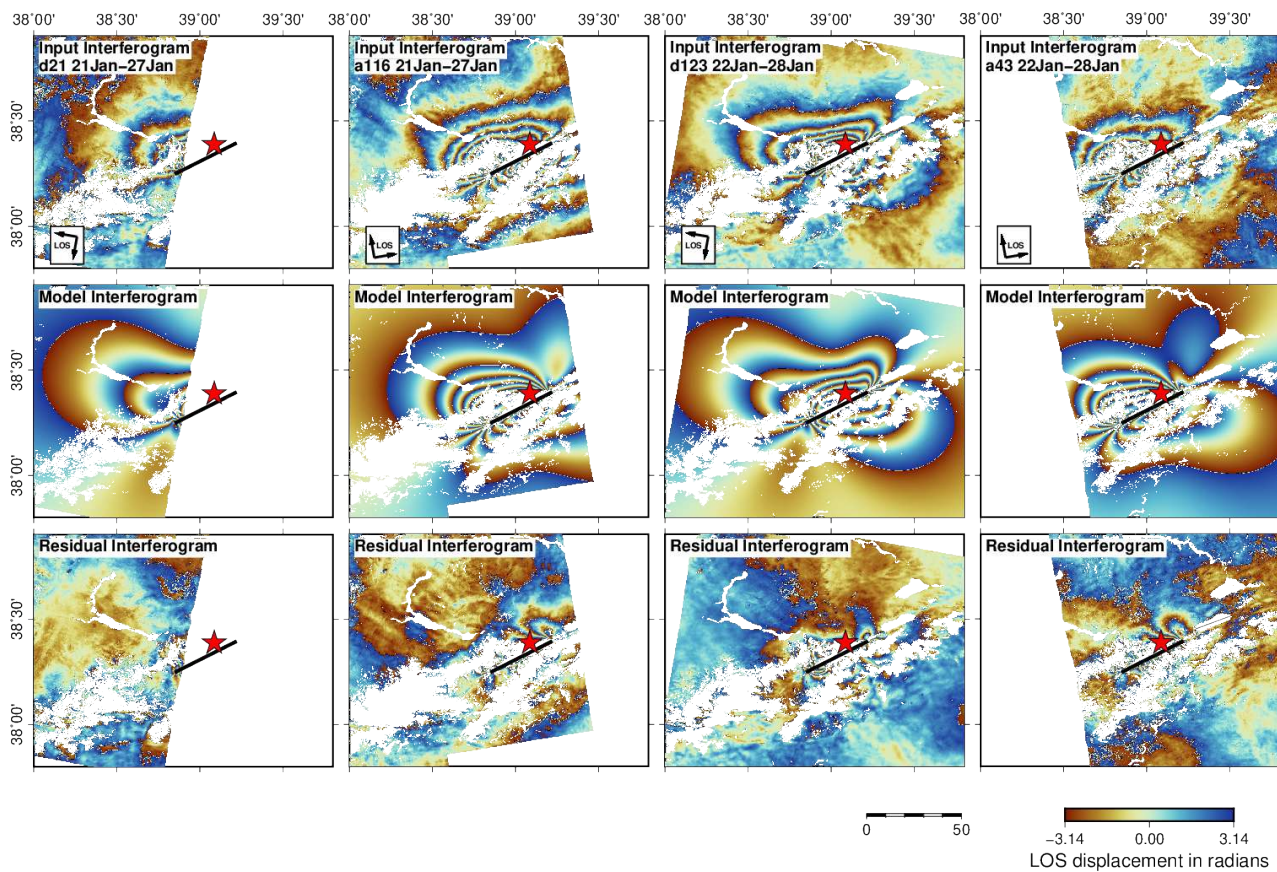
**Figure S2.** Observed Sentinel-1 interferograms on (left to right) tracks 21D, 116A, 123D, 43A. Middle: synthetic interferograms based on uniform slip on a single model fault plane (see parameters in Table S7). The thick black line is the model fault surface projections and the red star is the mainshock hypocenter. Bottom: residual interferograms.

March 25, 2020, 9:12pm
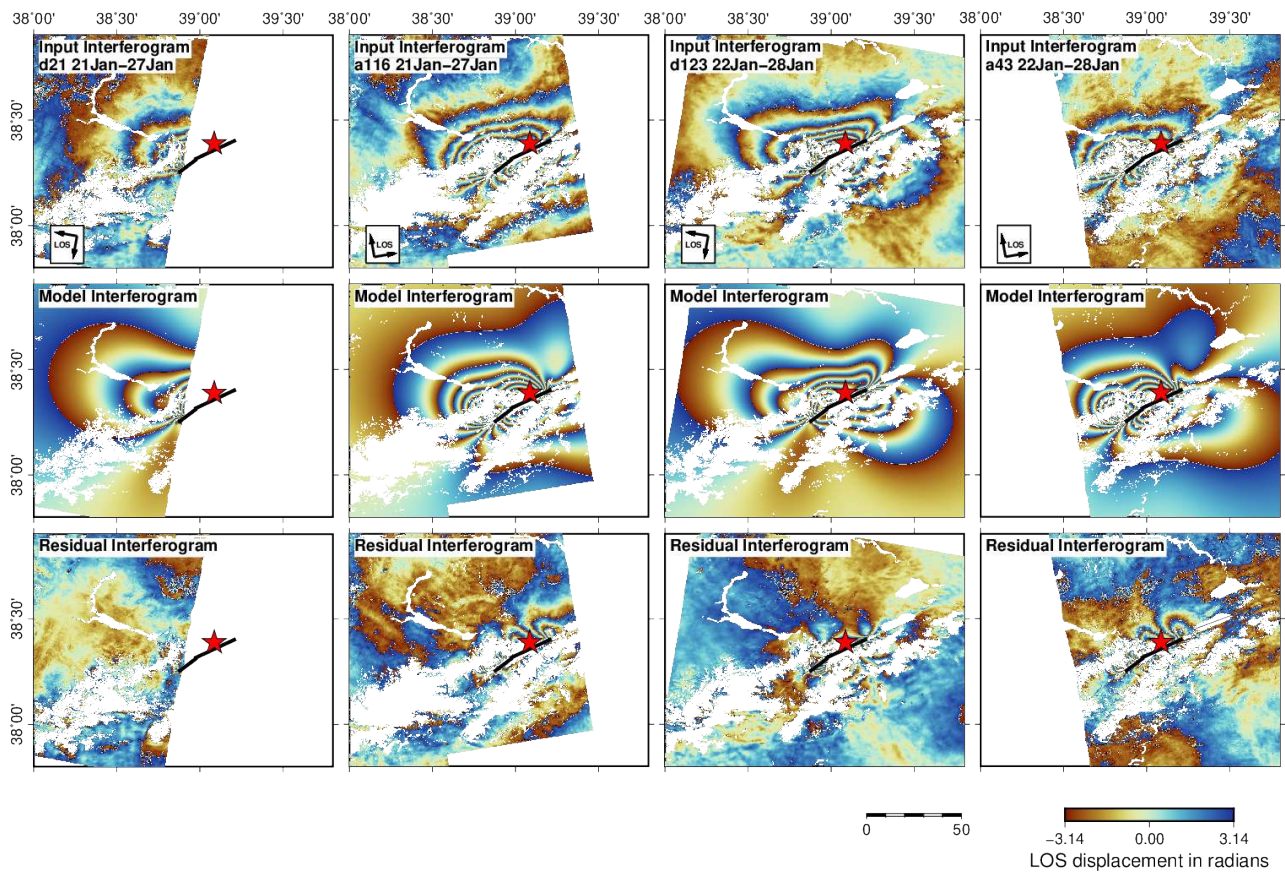
**Figure S3.** Observed Sentinel-1 interferograms on (left to right) tracks 21D, 116A, 123D, 43A. Middle: synthetic interferograms based on uniform slip on two model fault planes drawn from the the mapped trace of the EAF (Duman & Emre, 2013) (see parameters in Table S8). Thick black lines show surface projections of the model faults and the red star is the mainshock hypocenter. Bottom: residual interferograms.
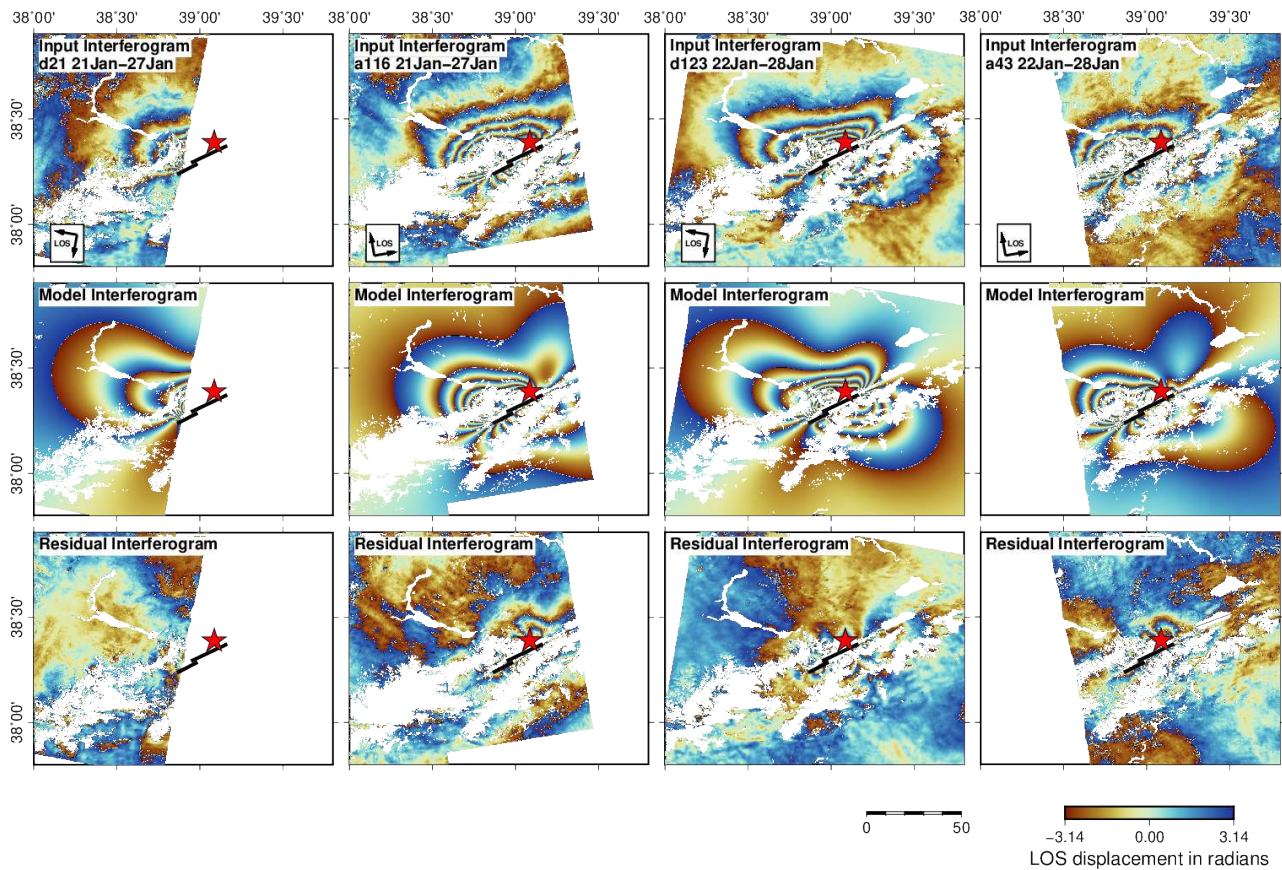
**Figure S4.** Observed Sentinel-1 interferograms on (left to right) tracks 21D, 116A, 123D, 43A. Middle: synthetic interferograms based on uniform slip on two model fault planes (see parameters in Table S8). Thick black lines show surface projections of the model faults and the red star is the mainshock hypocenter. Bottom: residual interferograms.
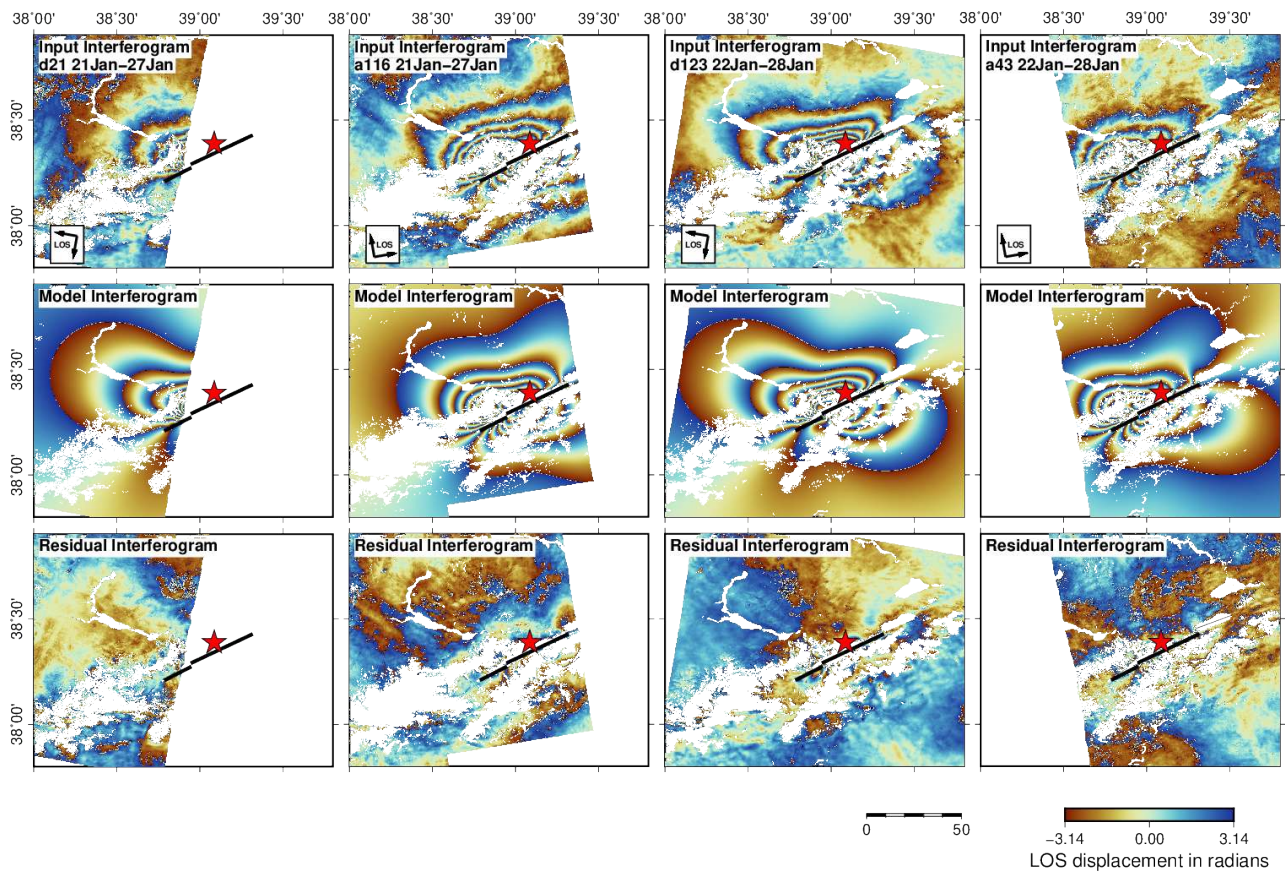
**Figure S5.** Observed Sentinel-1 interferograms on (left to right) tracks 21D, 116A, 123D, 43A. Middle: synthetic interferograms based on variable slip and uniform rake on two model fault planes. We used the strike, rake, dip and fault positions obtained in Table S8. Thick black lines show surface projections of the model faults and the red star is the mainshock hypocenter. Bottom: residual interferograms.
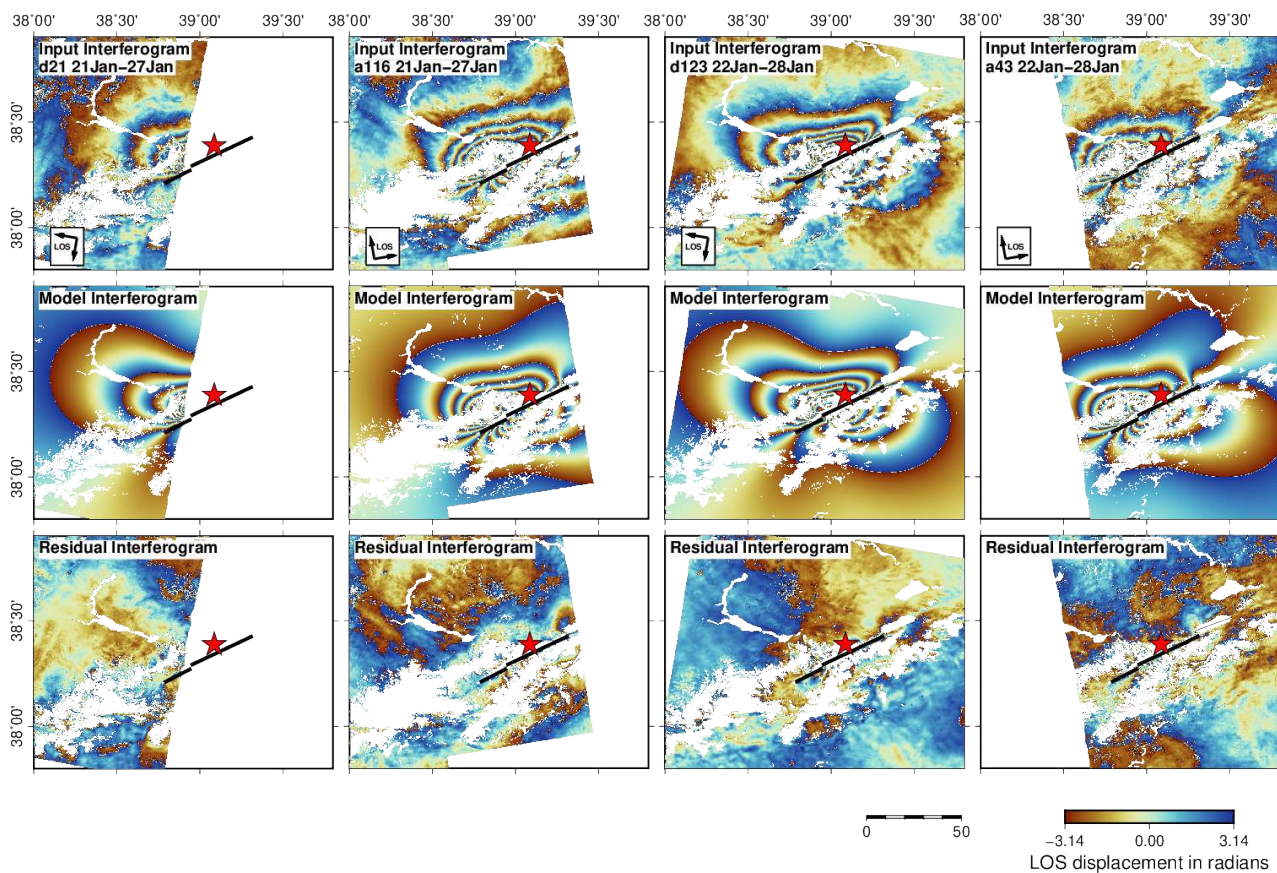
**Figure S6.** Top: Observed Sentinel-1 interferograms on (left to right) tracks 21D, 116A, 123D, 43A. Middle: equivalent synthetic interferograms based on variable slip and rake on two model fault planes. We used the strike, dip and fault positions obtained in Table S8; the fault slip model is shown in Figure S7. Thick black lines show surface projections of the model faults and the red star is the mainshock hypocenter. Bottom: residual interferograms.
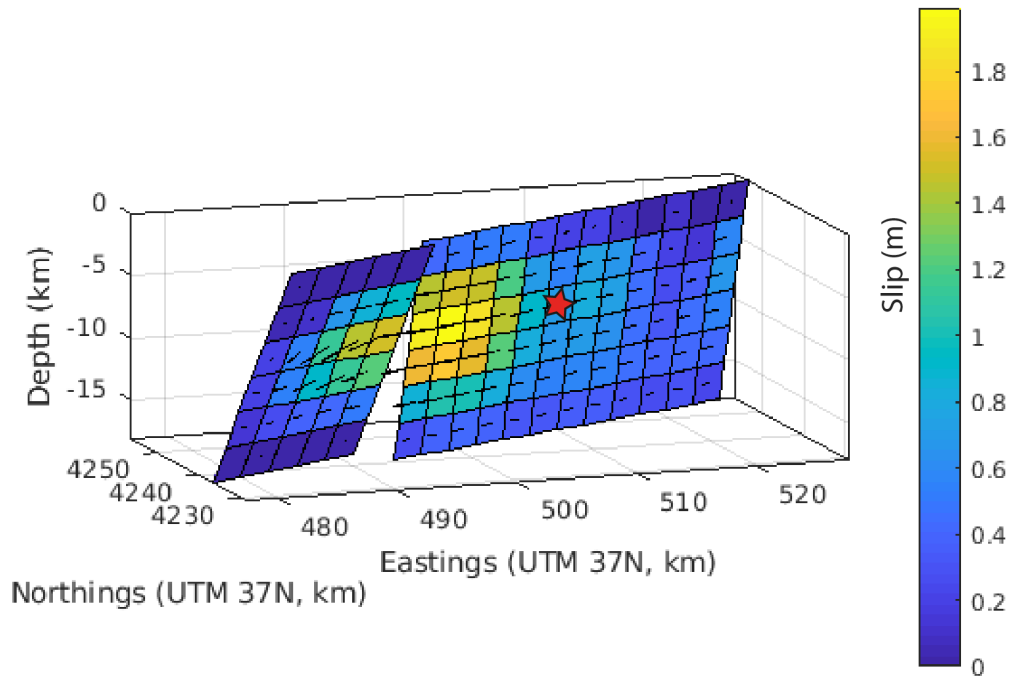
**Figure S7.** Modeled slip distribution with variable rake. Model fault patches measure $3 \times 3$ km. The red star is the relocated mainshock hypocenter at 8 km focal depth projected on the fault plane.
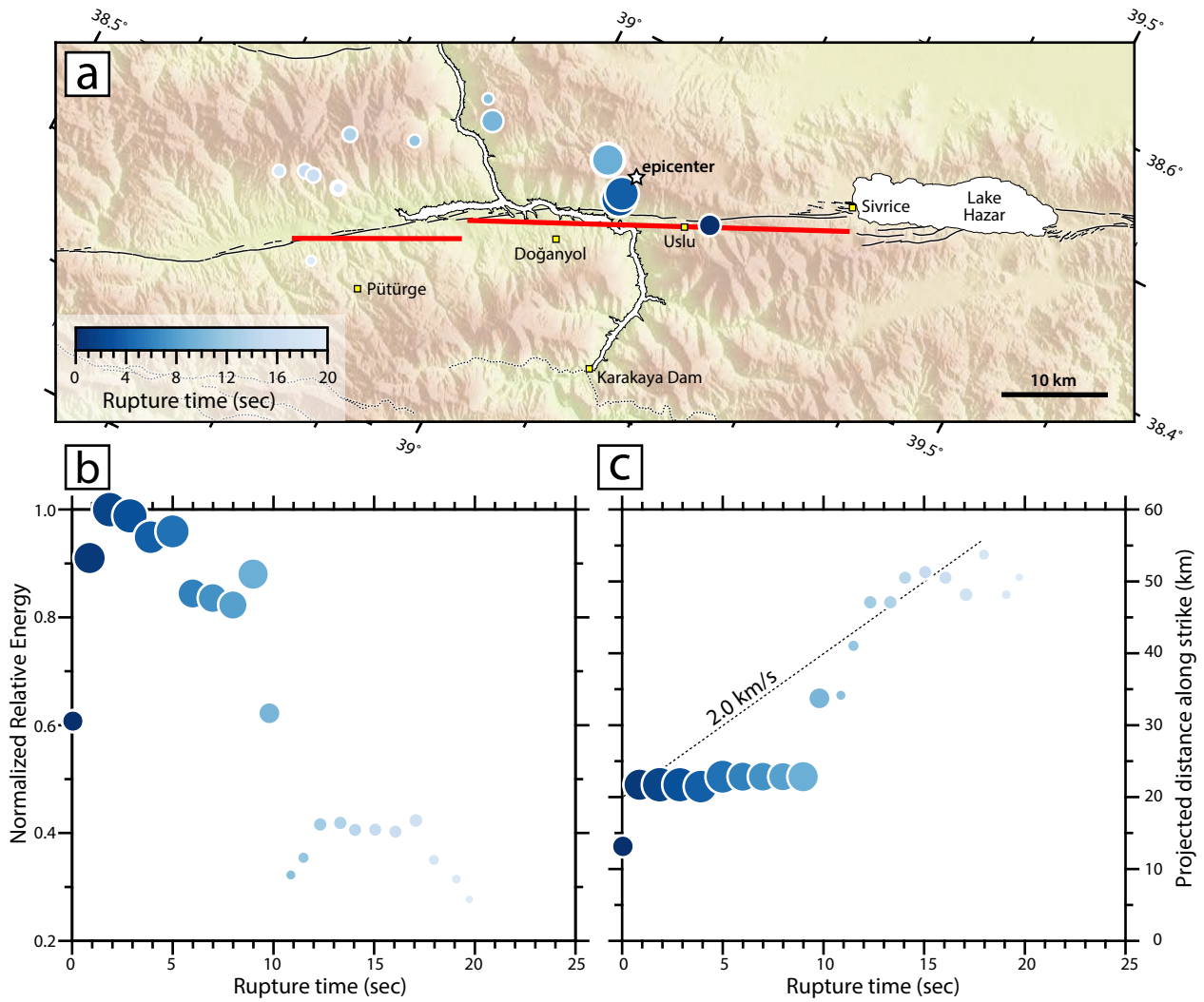
**Figure S8.** Back projection results. (a) Back projection sub-events in map view, scaled by relative energy and colored by rupture time. Thick red lines are surface projections of our preferred InSAR model faults for the 2020 Elazığ mainshock. Thin black lines show active faults as in Figure 1b–c of the main paper. (b) Sub-event relative energy versus rupture time. (c) Sub-event distance along strike versus rupture time. Distances are projected onto a line of strike 244°, with 0 km marking the eastern end of the InSAR model fault.
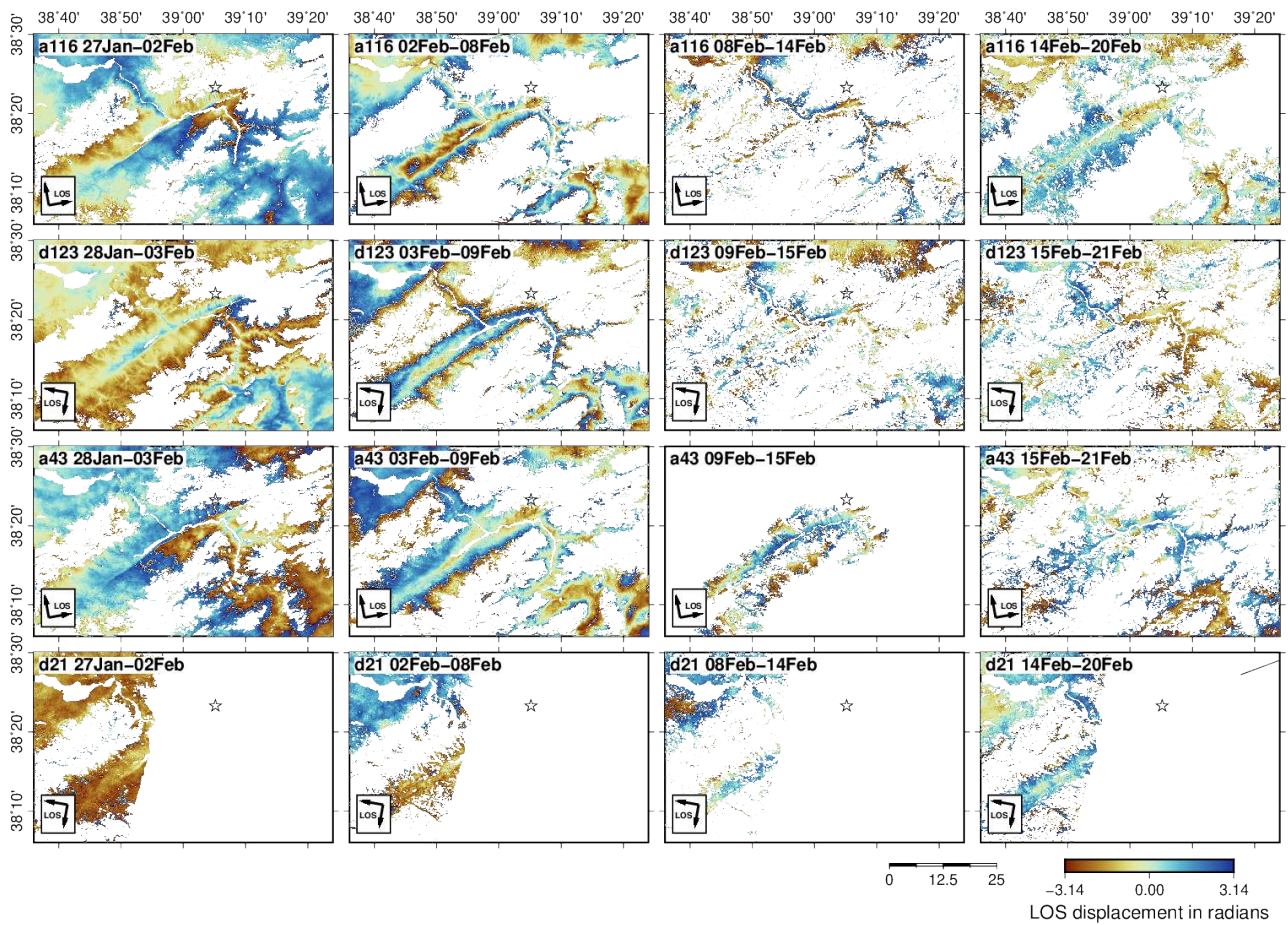
**Figure S9.** Re-wrapped 6 day interferograms along the Pütürge segment of the EAF. From top to bottom, we plot tracks A116, D123, A43 and D21. From left to right, we plot interferograms in chronological order; for example for track A116 we plot January 27–February 2, February 2–8, February 8–14, and February 14–20 interferograms.
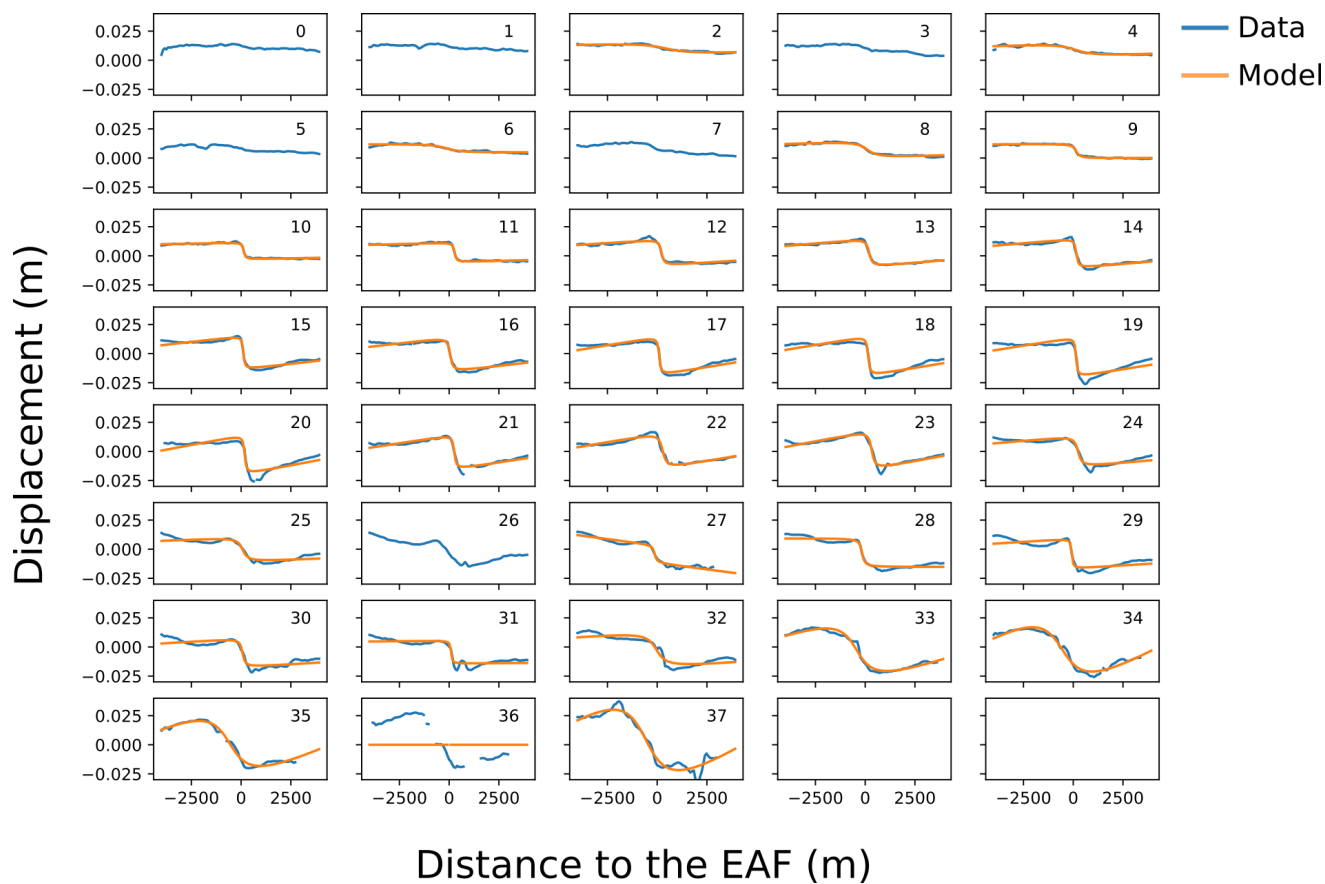
**Figure S10.** For each plot, blue line is the projected displacements onto the 244°-oriented fault sampled along the profiles across the EAF. The orange line is the best fit to our afterslip model. Numbers in each plot correspond to the profile numbers plotted in Figure 4. Plots without orange line couldn't be fitted by our model.
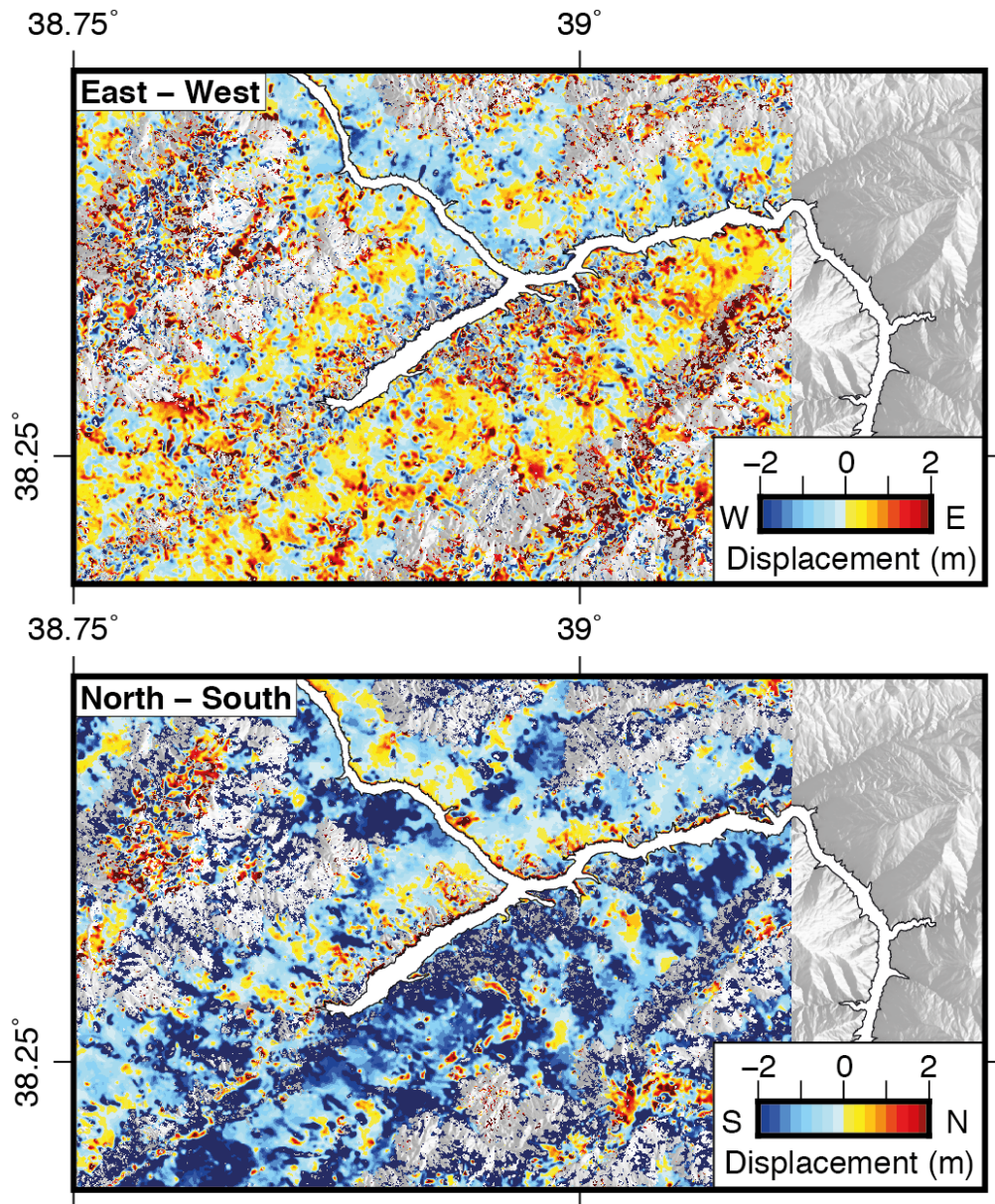
**Figure S11.** Horizontal coseismic–early postseismic displacements mapped using an optical image correlation (OIC) of ESA Sentinel-2 images. The pre-event image was acquired on November 9 2019 and the post-event image was collected on February 27 2020. The top panel is the E–W displacement field and the lower panel is the N–S displacement field.

March 25, 2020, 9:12pm

**Table S1.** SAR image acquisition dates used in this study. All dates are in 2020.

| Track | Pass1 | Pass 2 | Pass3 | Pass4 | Pass5 | Pass6 |
|---|---|---|---|---|---|---|
| $116A$ | 21 January | 27 January | 02 February | 08 February | 14 February | 20 February |
| $43A$ | 22 January | 28 January | 03 February | 09 February | 15 February | 21 February |
| $21D$ | 21 January | 27 January | 02 February | 08 February | 14 February | 20 February |
| $123D$ | 22 January | 28 January | 03 February | 09 February | 15 February | 21 February |

**Table S2.** Calibrated hypocenters in the Sivrice background seismicity cluster. Here, direct calibration was achieved with data from epicentral distances of $<0.8°$ and the 90% hypocentroid uncertainty is 0.8 km. Date is written year.month.day, Time is in UTC, and Lat and Lon are latitude and longitude in degrees N and E. Depth is focal depth in kilometers, with superscript codes that describe the source of the depth constraint: $f$ for free-depth solutions, $n$ for near-source station readings, and $l$ for local-source station readings. Mag is the magnitude taken from the ISC bulletin, A1 is the azimuth of the 90% confidence ellipse in degrees clockwise from north, L1 and L2 are semi-axis lengths of the confidence ellipse in kilometers, and Area is the area of the 90% confidence ellipse in $km^2$.

| Date | Time | Lat | Lon | Depth | Mag | A1 | L1 | L2 | Area |
|------|------|-----|-----|-------|-----|----|----|----|------|
| 1998.3.28 | 0:29:58.12 | 38.25557 | 38.75876 | $10.00^l$ | $m_b$ 4.6 | 287 | 1.11 | 1.31 | 4.6 |
| 1998.5.9 | 15:38:0.96 | 38.35068 | 38.93081 | $15.00^l$ | $m_b$ 4.9 | 88 | 0.88 | 1.06 | 3.0 |
| 1999.4.13 | 9:47:2.41 | 38.55251 | 39.23861 | $11.00^l$ | $m_b$ 4.3 | 51 | 1.35 | 1.81 | 7.7 |
| 2000.5.7 | 23:10:54.48 | 38.21077 | 38.81838 | $17.00^l$ | $m_b$ 4.4 | 277 | 1.35 | 1.52 | 6.4 |
| 2000.5.22 | 19:48:49.19 | 38.33493 | 39.38739 | $4.00^l$ | $m_b$ 4.3 | 306 | 1.42 | 1.88 | 8.4 |
| 2003.7.13 | 1:48:22.32 | 38.35173 | 38.94461 | $17.00^l$ | $m_b$ 5.3 | 65 | 0.83 | 0.92 | 2.4 |
| 2003.8.20 | 2:51:3.42 | 38.27225 | 38.86599 | $9.00^l$ | $m_b$ 4.1 | 270 | 1.15 | 1.54 | 5.6 |
| 2003.8.20 | 9:14:44.77 | 38.25428 | 38.85186 | $12.00^l$ | $m_b$ 4.3 | 39 | 1.20 | 1.43 | 5.4 |
| 2004.1.6 | 10:39:11.39 | 38.30099 | 39.00507 | $9.00^l$ | $m_b$ 4.5 | 29 | 1.01 | 1.23 | 3.9 |
| 2004.8.11 | 15:48:24.55 | 38.41631 | 39.23305 | $10.00^l$ | $m_b$ 5.3 | 65 | 0.83 | 0.95 | 2.5 |
| 2004.8.13 | 20:35:5.88 | 38.41625 | 39.19980 | $9.00^l$ | $m_b$ 4.3 | 53 | 1.08 | 1.31 | 4.4 |
| 2004.8.14 | 0:20:26.02 | 38.44206 | 39.22990 | $8.00^l$ | $m_b$ 4.3 | 50 | 1.18 | 1.48 | 5.5 |
| 2004.8.14 | 20:42:16.34 | 38.44412 | 39.18468 | $10.00^l$ | $m_b$ 4.4 | 59 | 1.18 | 1.41 | 5.2 |
| 2005.11.26 | 15:56:55.07 | 38.31216 | 38.84697 | $11.00^l$ | $m_b$ 5.1 | 68 | 0.86 | 0.91 | 2.5 |
| 2005.12.28 | 14:8:0.06 | 38.51166 | 39.31948 | $8.00^l$ | $m_b$ 4.2 | 71 | 1.20 | 1.63 | 6.1 |
| 2007.1.3 | 23:17:8.22 | 38.03255 | 38.78145 | $13.00^l$ | $m_b$ 3.5 | 37 | 0.98 | 1.29 | 4.0 |
| 2007.2.3 | 18:22:27.80 | 38.03248 | 38.77706 | $9.00^l$ | $m_b$ 3.5 | 8 | 1.33 | 1.49 | 6.2 |
| 2007.2.9 | 2:22:56.06 | 38.40347 | 39.08406 | $9.00^l$ | $m_b$ 5.2 | 68 | 0.81 | 0.95 | 2.4 |
| 2007.2.11 | 3:43:0.55 | 38.42330 | 39.12568 | $10.00^l$ | $m_b$ 3.8 | 54 | 1.10 | 1.56 | 5.4 |
| 2007.2.11 | 17:51:40.50 | 38.38416 | 39.20979 | $6.00^l$ | $m_b$ 4.1 | 55 | 1.08 | 1.50 | 5.1 |
| 2007.2.21 | 11:5:27.65 | 38.39213 | 39.28718 | $16.00^n$ | $m_b$ 5.5 | 64 | 0.79 | 0.92 | 2.3 |
| 2007.2.23 | 12:12:0.46 | 38.38210 | 39.30872 | $11.00^l$ | $m_b$ 3.4 | 57 | 1.25 | 1.47 | 5.8 |
| 2007.2.25 | 15:14:30.14 | 38.45385 | 39.25169 | $9.00^l$ | $m_b$ 3.3 | 13 | 1.75 | 1.82 | 10.0 |
| 2007.2.28 | 19:32:23.80 | 38.37386 | 39.23048 | $12.00^l$ | – | 25 | 1.08 | 1.28 | 4.3 |
| 2007.2.28 | 19:55:31.76 | 38.33326 | 39.25524 | $8.00^l$ | $m_b$ 4.7 | 57 | 0.93 | 1.09 | 3.2 |
| 2007.2.28 | 20:8:10.32 | 38.33620 | 39.22073 | $11.00^l$ | $m_b$ 3.5 | 51 | 1.14 | 1.30 | 4.7 |
| 2007.2.28 | 23:27:46.86 | 38.37593 | 39.26604 | $13.00^l$ | $m_b$ 4.6 | 48 | 0.92 | 1.08 | 3.1 |

March 25, 2020, 9:12pm

| Date | Time | Lat | Lon | Depth | Mag | A1 | L1 | L2 | Area |
|------|------|-----|-----|-------|-----|----|----|----|----|
| 2007.3.7 | 0:17:32.43 | 38.06177 | 38.77855 | $9.00^l$ | $m_b$ 3.7 | 38 | 1.26 | 1.53 | 6.0 |
| 2007.3.11 | 23:35:27.85 | 38.37103 | 39.31627 | $13.00^l$ | $m_b$ 3.6 | 49 | 0.94 | 1.11 | 3.3 |
| 2007.4.14 | 4:30:37.48 | 38.32023 | 39.31332 | $9.00^l$ | $m_b$ 4.2 | 48 | 0.91 | 1.10 | 3.1 |
| 2009.3.22 | 2:31:53.51 | 38.34052 | 38.94328 | $12.00^n$ | – | 69 | 1.14 | 1.34 | 4.8 |
| 2009.5.10 | 1:36:32.25 | 38.19693 | 38.61461 | $13.00^l$ | – | 47 | 1.06 | 1.45 | 4.8 |
| 2009.5.26 | 2:1:34.02 | 38.73082 | 39.45964 | $11.00^n$ | $m_b$ 3.5 | 46 | 1.08 | 1.31 | 4.4 |
| 2009.6.11 | 14:30:10.10 | 38.35704 | 38.95518 | $14.00^n$ | – | 56 | 1.06 | 1.21 | 4.0 |
| 2009.7.7 | 15:57:2.50 | 38.25384 | 38.74815 | $12.00^l$ | $m_b$ 4.3 | 59 | 0.80 | 0.92 | 2.3 |
| 2009.8.12 | 20:23:27.55 | 38.25721 | 38.75500 | $8.00^l$ | $m_b$ 3.8 | 31 | 0.92 | 1.03 | 3.0 |
| 2009.10.5 | 1:58:9.07 | 38.35162 | 39.23425 | $15.00^l$ | $m_b$ 3.4 | 286 | 1.22 | 1.53 | 5.9 |
| 2009.10.28 | 4:27:0.52 | 38.18440 | 38.50730 | $13.00^l$ | – | 31 | 1.12 | 1.43 | 5.0 |
| 2010.3.5 | 20:37:52.12 | 38.37140 | 39.36256 | $13.00^l$ | – | 273 | 1.06 | 1.51 | 5.0 |
| 2010.3.18 | 2:58:38.25 | 38.65619 | 39.66380 | $14.00^l$ | – | 315 | 1.26 | 1.64 | 6.5 |
| 2010.9.17 | 10:17:6.05 | 38.12873 | 39.00035 | $13.00^l$ | $m_b$ 4.7 | 72 | 0.80 | 0.98 | 2.5 |
| 2010.10.28 | 22:40:16.20 | 38.39175 | 39.02796 | $12.00^n$ | – | 29 | 1.08 | 1.32 | 4.5 |
| 2011.2.3 | 15:27:49.04 | 38.45134 | 39.20053 | $10.00^l$ | $m_b$ 3.8 | 338 | 1.02 | 1.12 | 3.6 |
| 2011.2.4 | 11:21:58.73 | 38.10144 | 38.56895 | $11.00^l$ | – | 51 | 1.06 | 1.31 | 4.3 |
| 2011.3.11 | 2:51:53.27 | 38.25858 | 38.60640 | $9.00^l$ | – | 293 | 1.01 | 1.32 | 4.2 |
| 2011.4.18 | 10:53:29.76 | 38.14809 | 38.46590 | $10.00^l$ | – | 79 | 1.16 | 1.51 | 5.5 |
| 2011.6.23 | 7:34:43.44 | 38.58784 | 39.62203 | $13.00^l$ | $m_b$ 5.2 | 75 | 0.78 | 0.91 | 2.2 |
| 2011.6.23 | 12:0:6.00 | 38.58126 | 39.61414 | $11.00^l$ | – | 37 | 1.20 | 1.45 | 5.5 |
| 2011.6.26 | 20:16:1.26 | 38.55915 | 39.59563 | $10.00^l$ | – | 43 | 1.09 | 1.23 | 4.2 |
| 2011.7.1 | 8:53:47.55 | 38.60904 | 39.64224 | $11.00^l$ | – | 332 | 1.23 | 1.35 | 5.2 |
| 2011.7.2 | 22:0:59.68 | 38.59802 | 39.63874 | $11.00^l$ | – | 312 | 1.10 | 1.26 | 4.4 |
| 2011.7.22 | 21:20:38.23 | 38.57685 | 39.63369 | $13.00^l$ | $m_b$ 3.6 | 85 | 0.87 | 0.96 | 2.6 |
| 2011.8.4 | 3:13:8.62 | 38.59617 | 39.64758 | $11.00^l$ | $m_b$ 4.1 | 30 | 0.98 | 1.06 | 3.3 |
| 2011.10.10 | 7:14:31.38 | 38.46125 | 39.24347 | $11.00^n$ | $m_b$ 4.0 | 1 | 1.29 | 1.41 | 5.7 |
| 2011.11.19 | 8:8:55.23 | 38.10023 | 38.71107 | $11.00^l$ | – | 67 | 0.94 | 1.16 | 3.4 |
| 2011.12.1 | 2:12:23.35 | 38.45094 | 39.12751 | $13.00^n$ | – | 286 | 1.04 | 1.18 | 3.9 |
| 2012.3.21 | 23:17:17.25 | 38.63535 | 39.64311 | $11.00^l$ | $M_L$ 2.8 | 324 | 1.18 | 1.51 | 5.6 |
| 2012.4.10 | 16:40:33.62 | 38.12730 | 39.02894 | $11.00^l$ | – | 89 | 1.04 | 1.13 | 3.7 |
| 2012.4.15 | 10:30:46.52 | 38.60220 | 39.61199 | $18.00^l$ | – | 313 | 1.33 | 1.57 | 6.6 |
| 2012.5.8 | 22:37:29.89 | 38.36512 | 38.84361 | $13.00^n$ | $m_b$ 3.4 | 275 | 0.93 | 1.10 | 3.2 |
| 2012.5.9 | 3:3:49.84 | 38.83272 | 39.06833 | $12.00^l$ | – | 346 | 1.02 | 1.18 | 3.8 |
| 2012.5.12 | 23:58:6.38 | 38.59000 | 39.58759 | $15.00^l$ | – | 72 | 1.27 | 1.86 | 7.4 |
| 2012.5.14 | 17:51:8.49 | 38.56421 | 39.51558 | $14.00^l$ | – | 68 | 1.02 | 1.08 | 3.4 |
| 2012.5.14 | 22:23:11.06 | 38.38433 | 39.01788 | $12.00^n$ | – | 275 | 1.02 | 1.10 | 3.5 |
| 2012.5.15 | 6:55:5.47 | 38.56716 | 39.52540 | $12.00^l$ | – | 282 | 1.42 | 1.51 | 6.8 |
| 2012.5.25 | 11:22:39.58 | 38.14025 | 38.58633 | $11.00^l$ | $m_b$ 4.2 | 87 | 0.84 | 0.99 | 2.6 |
| 2012.5.25 | 13:19:39.49 | 38.14800 | 38.61311 | $11.00^l$ | – | 70 | 0.99 | 1.28 | 4.0 |
| 2012.6.25 | 5:59:56.03 | 38.62756 | 39.63630 | $14.00^l$ | – | 329 | 1.10 | 1.25 | 4.3 |
| 2012.7.5 | 16:56:26.83 | 38.93663 | 38.93621 | $8.00^l$ | $M_L$ 3.0 | 31 | 1.21 | 1.45 | 5.5 |
| 2013.8.28 | 6:26:8.88 | 38.38142 | 38.90818 | $15.00^n$ | $m_b$ 3.7 | 271 | 0.89 | 1.05 | 2.9 |

| Date | Time | Lat | Lon | Depth | Mag | A1 | L1 | L2 | Area |
|---|---|---|---|---|---|---|---|---|---|
| 2014.3.26 | 14:0:14.75 | 38.13192 | 38.56165 | $12.00^l$ | $m_b$ 3.9 | 66 | 0.97 | 1.18 | 3.6 |
| 2014.9.20 | 3:9:38.98 | 38.42010 | 39.24860 | $12.00^n$ | – | 80 | 0.94 | 1.15 | 3.4 |
| 2014.10.20 | 15:45:7.57 | 38.17462 | 38.66256 | $13.00^l$ | – | 80 | 0.87 | 1.06 | 2.9 |
| 2015.10.3 | 21:8:3.36 | 38.17535 | 38.93047 | $15.00^l$ | $m_b$ 3.9 | 66 | 0.83 | 0.99 | 2.6 |
| 2017.10.26 | 22:42:23.20 | 38.39476 | 39.04312 | $10.00^l$ | $M_w$ 3.8 | 65 | 0.85 | 1.01 | 2.7 |
| 2018.1.19 | 13:53:13.29 | 38.25993 | 38.79618 | $14.00^l$ | $M_L$ 4.0 | 18 | 1.03 | 1.18 | 3.8 |
| 2019.2.22 | 18:1:0.05 | 38.29817 | 38.78999 | $11.00^l$ | $M_w$ 3.7 | 30 | 1.10 | 1.22 | 4.2 |
| 2019.4.4 | 17:31:7.95 | 38.36734 | 39.13332 | $8.00^n$ | $m_b$ 5.1 | 70 | 0.84 | 0.97 | 2.6 |
| 2019.12.27 | 7:2:25.86 | 38.35516 | 39.02047 | $15.00^l$ | $m_b$ 5.0 | 66 | 0.75 | 0.89 | 2.1 |
| 2020.1.24 | 17:55:11.08 | 38.38837 | 39.08573 | $8.00^l$ | $M_w$ 6.7 | 79 | 0.84 | 1.11 | 2.9 |

**Table S3.** Calibrated hypocenters of the Sivrice foreshock–aftershock cluster, where direct calibration was achieved with data from epicentral distances of <0.8° and the 90% hypocentroid uncertainty is 0.7 km. Columns are as in Table S2.

| Date | Time | Lat | Lon | Depth | Mag | A1 | L1 | L2 | Area |
|---|---|---|---|---|---|---|---|---|---|
| 2019.2.15 | 17:49:32.54 | 38.29580 | 38.78067 | $11.00^l$ | $M_w$ 3.0 | 74 | 1.10 | 1.36 | 4.7 |
| 2019.2.20 | 13:56:39.75 | 37.61710 | 38.46714 | $13.00^l$ | $M_w$ 3.3 | 87 | 0.79 | 0.93 | 2.3 |
| 2019.2.22 | 18:0:59.84 | 38.30354 | 38.81841 | $12.00^l$ | $M_w$ 3.7 | 51 | 1.10 | 1.26 | 4.3 |
| 2019.2.23 | 2:41:14.50 | 37.62072 | 38.51587 | $11.00^l$ | $M_w$ 3.3 | 290 | 1.04 | 1.24 | 4.1 |
| 2019.2.28 | 8:33:41.90 | 38.63966 | 39.63761 | $17.00^l$ | $M_L$ 3.0 | 272 | 1.29 | 1.55 | 6.3 |
| 2019.3.13 | 11:59:31.79 | 38.76130 | 39.98296 | $17.00^n$ | $M_w$ 3.5 | 291 | 1.05 | 1.36 | 4.5 |
| 2019.4.2 | 7:39:37.17 | 37.46722 | 38.60297 | $15.00^n$ | $M_w$ 3.3 | 281 | 0.96 | 1.15 | 3.5 |
| 2019.4.4 | 17:31:7.95 | 38.38319 | 39.13927 | $11.00^n$ | $m_b$ 5.1 | 77 | 0.78 | 0.93 | 2.3 |
| 2019.4.4 | 17:55:41.61 | 38.41286 | 39.13435 | $11.00^n$ | $M_L$ 3.3 | 275 | 1.07 | 1.18 | 4.0 |
| 2019.4.4 | 18:58:54.24 | 38.42347 | 39.12951 | $13.00^n$ | $M_L$ 3.0 | 75 | 0.98 | 1.12 | 3.4 |
| 2019.4.4 | 23:1:37.70 | 38.40593 | 39.10089 | $10.00^n$ | $M_L$ 2.1 | 273 | 1.21 | 1.41 | 5.3 |
| 2019.4.5 | 2:2:21.37 | 38.42455 | 39.12639 | $13.00^n$ | $M_L$ 1.6 | 276 | 1.44 | 1.63 | 7.4 |
| 2019.4.5 | 3:57:1.37 | 38.41525 | 39.11979 | $13.00^l$ | $M_L$ 2.3 | 55 | 1.03 | 1.19 | 3.8 |
| 2019.4.5 | 4:58:48.42 | 38.39903 | 39.08013 | $13.00^l$ | $M_L$ 2.6 | 61 | 1.01 | 1.13 | 3.6 |
| 2019.4.5 | 13:33:40.63 | 38.40943 | 39.14155 | $11.00^n$ | $M_L$ 2.6 | 281 | 0.91 | 1.11 | 3.2 |
| 2019.4.5 | 13:45:54.37 | 38.43008 | 39.12765 | $14.00^n$ | $M_L$ 1.9 | 292 | 1.28 | 1.73 | 7.0 |
| 2019.4.6 | 22:37:43.33 | 38.43503 | 39.16592 | $10.00^n$ | $M_L$ 2.3 | 282 | 1.42 | 1.82 | 8.1 |
| 2019.4.8 | 2:23:33.09 | 38.41214 | 39.09027 | $13.00^n$ | $M_L$ 2.6 | 75 | 0.99 | 1.12 | 3.5 |
| 2019.4.8 | 9:46:33.75 | 38.39662 | 39.07968 | $13.00^l$ | $M_L$ 3.7 | 80 | 0.94 | 1.18 | 3.5 |
| 2019.4.9 | 2:50:58.59 | 38.39372 | 39.11173 | $11.00^n$ | $M_L$ 2.4 | 52 | 1.36 | 1.81 | 7.7 |
| 2019.4.9 | 13:28:18.43 | 38.42211 | 39.11866 | $14.00^n$ | $M_L$ 2.3 | 8 | 1.29 | 1.56 | 6.3 |
| 2019.4.9 | 17:18:4.07 | 38.18987 | 38.55556 | $16.00^n$ | $M_w$ 3.3 | 31 | 1.03 | 1.13 | 3.7 |
| 2019.4.9 | 17:38:27.04 | 38.18642 | 38.57746 | $13.00^n$ | $M_L$ 2.2 | 38 | 1.12 | 1.27 | 4.4 |
| 2019.4.10 | 17:1:36.06 | 38.42430 | 39.10788 | $14.00^n$ | $M_L$ 3.0 | 27 | 1.08 | 1.15 | 3.9 |
| 2019.4.12 | 17:3:24.10 | 38.45090 | 39.29827 | $14.00^n$ | $M_L$ 2.8 | 63 | 1.15 | 1.46 | 5.2 |
| 2019.4.14 | 22:44:27.12 | 38.45872 | 39.24957 | $14.00^n$ | $M_L$ 3.3 | 86 | 0.84 | 1.13 | 3.0 |
| 2019.4.16 | 17:47:57.73 | 38.45013 | 39.20266 | $13.00^n$ | $M_L$ 3.7 | 271 | 1.22 | 1.30 | 5.0 |
| 2019.4.16 | 18:15:20.95 | 38.51697 | 39.31115 | $13.00^n$ | $M_L$ 3.0 | 52 | 1.18 | 1.40 | 5.2 |
| 2019.4.20 | 1:39:27.94 | 38.46634 | 39.26543 | $14.00^n$ | $M_w$ 3.6 | 68 | 1.17 | 1.35 | 5.0 |
| 2019.4.20 | 14:12:32.46 | 38.49815 | 39.30953 | $10.00^l$ | $M_L$ 2.5 | 81 | 1.21 | 1.48 | 5.6 |
| 2019.4.22 | 22:8:32.54 | 38.37045 | 39.03440 | $11.00^l$ | $M_L$ 2.8 | 355 | 1.17 | 1.29 | 4.7 |
| 2019.4.23 | 2:12:58.79 | 38.47241 | 39.29015 | $13.00^n$ | $M_L$ 3.4 | 87 | 0.91 | 1.14 | 3.3 |
| 2019.5.2 | 15:4:13.11 | 38.46627 | 39.29882 | $12.00^l$ | $M_L$ 2.8 | 68 | 0.99 | 1.36 | 4.3 |
| 2019.5.5 | 11:15:0.66 | 38.82279 | 38.83126 | $11.00^l$ | $M_L$ 2.2 | 290 | 1.53 | 1.81 | 8.7 |
| 2019.5.6 | 1:0:37.08 | 38.40657 | 39.11178 | $13.00^n$ | $M_L$ 2.0 | 276 | 1.44 | 1.61 | 7.3 |
| 2019.5.20 | 17:16:48.20 | 38.43055 | 39.11957 | $13.00^n$ | $M_L$ 3.2 | 73 | 1.25 | 1.55 | 6.1 |
| 2019.5.26 | 23:36:2.55 | 38.36386 | 38.80922 | $14.00^n$ | $M_L$ 2.2 | 67 | 1.12 | 1.58 | 5.6 |
| 2019.6.3 | 6:47:11.33 | 38.53098 | 39.34602 | $8.00^l$ | $M_L$ 3.2 | 87 | 1.13 | 1.24 | 4.4 |
| 2019.6.8 | 11:12:33.86 | 38.36170 | 38.96350 | $13.00^n$ | $M_L$ 2.6 | 45 | 1.18 | 1.30 | 4.8 |
| 2019.6.25 | 11:20:3.71 | 38.37053 | 38.78376 | $13.00^n$ | $M_L$ 2.5 | 56 | 1.19 | 1.53 | 5.7 |
| 2019.6.30 | 22:1:57.34 | 37.57708 | 38.80755 | $13.00^l$ | $M_L$ 2.4 | 275 | 0.96 | 1.18 | 3.6 |

| Date | Time | Lat | Lon | Depth | Mag | A1 | L1 | L2 | Area |
|---|---|---|---|---|---|---|---|---|---|
| 2019.7.1 | 23:16:38.17 | 37.52735 | 38.71427 | $12.00^l$ | $M_L$ 2.2 | 314 | 1.03 | 1.31 | 4.2 |
| 2019.7.27 | 0:51:47.49 | 37.22215 | 38.08781 | $12.00^l$ | $M_L$ 2.5 | 277 | 1.11 | 1.65 | 5.7 |
| 2019.8.16 | 22:4:52.12 | 38.40312 | 39.13982 | $11.00^n$ | $M_L$ 2.8 | 63 | 0.87 | 1.38 | 3.8 |
| 2019.8.19 | 1:30:30.90 | 38.88179 | 39.02837 | $7.00^l$ | $M_L$ 3.2 | 23 | 1.37 | 1.40 | 6.0 |
| 2019.9.1 | 18:51:43.66 | 38.79937 | 39.02605 | $8.00^l$ | $M_L$ 3.3 | 273 | 1.07 | 1.22 | 4.1 |
| 2019.9.20 | 1:43:21.21 | 38.50912 | 39.31533 | $12.00^l$ | $M_L$ 2.4 | 280 | 1.07 | 1.44 | 4.8 |
| 2019.9.28 | 12:29:52.59 | 38.66748 | 39.85797 | $10.00^n$ | $M_L$ 3.3 | 86 | 1.27 | 1.44 | 5.8 |
| 2019.9.30 | 5:36:30.86 | 37.47030 | 38.59613 | $14.00^n$ | $M_L$ 2.6 | 313 | 1.12 | 1.40 | 4.9 |
| 2019.10.2 | 4:36:28.26 | 38.45595 | 39.56694 | $12.00^n$ | $M_L$ 2.9 | 270 | 1.09 | 1.59 | 5.5 |
| 2019.11.3 | 16:34:42.14 | 38.35743 | 38.97069 | $15.00^n$ | $M_w$ 3.9 | 73 | 0.94 | 1.15 | 3.4 |
| 2019.11.4 | 7:16:3.30 | 37.50989 | 38.59503 | $9.00^l$ | $M_L$ 2.3 | 281 | 1.18 | 1.28 | 4.7 |
| 2019.11.7 | 21:28:48.02 | 37.66573 | 38.53568 | $14.00^l$ | $M_w$ 3.6 | 77 | 1.06 | 1.30 | 4.3 |
| 2019.11.13 | 20:33:7.30 | 37.66428 | 38.56301 | $15.00^n$ | $M_L$ 2.8 | 70 | 1.20 | 1.28 | 4.8 |
| 2019.11.22 | 0:55:17.36 | 38.38020 | 39.47867 | $12.00^n$ | $M_L$ 2.2 | 88 | 1.16 | 1.56 | 5.7 |
| 2019.12.27 | 7:2:25.61 | 38.37249 | 39.02873 | $17.00^l$ | $m_b$ 5.0 | 75 | 0.70 | 0.90 | 2.0 |
| 2020.1.24 | 17:55:10.69 | 38.39404 | 39.07740 | $9.00^l$ | $M_w$ 6.9 | 83 | 0.76 | 1.01 | 2.4 |
| 2020.1.24 | 18:8:5.18 | 38.41795 | 39.20520 | $12.00^n$ | $m_b$ 4.3 | 273 | 1.14 | 1.53 | 5.5 |
| 2020.1.24 | 18:32:35.41 | 38.40971 | 39.06650 | $11.00^n$ | $m_b$ 4.0 | 83 | 0.92 | 1.22 | 3.5 |
| 2020.1.24 | 18:43:22.73 | 38.42513 | 39.05247 | $10.00^c$ | $m_b$ 4.1 | 85 | 1.04 | 1.52 | 5.0 |
| 2020.1.24 | 19:3:7.73 | 38.30175 | 38.70466 | $15.00^l$ | $m_b$ 4.1 | 72 | 0.91 | 1.42 | 4.1 |
| 2020.1.24 | 19:49:38.16 | 38.40990 | 39.19191 | $7.00^n$ | $m_b$ 3.9 | 89 | 0.84 | 1.28 | 3.4 |
| 2020.1.24 | 20:45:3.62 | 38.40598 | 39.17785 | $8.00^n$ | $m_b$ 4.0 | 82 | 1.28 | 1.92 | 7.7 |
| 2020.1.25 | 0:48:50.76 | 38.48222 | 39.20738 | $12.00^n$ | $m_b$ 3.9 | 272 | 0.88 | 1.19 | 3.3 |
| 2020.1.25 | 0:57:17.65 | 38.35626 | 39.09423 | $12.00^l$ | $m_b$ 3.7 | 82 | 0.80 | 1.12 | 2.8 |
| 2020.1.25 | 1:2:35.85 | 38.38647 | 39.30001 | $10.00^c$ | $m_b$ 3.7 | 89 | 1.33 | 2.04 | 8.5 |
| 2020.1.25 | 6:7:33.00 | 38.34683 | 39.07728 | $11.00^n$ | $m_b$ 3.9 | 88 | 0.80 | 1.10 | 2.8 |
| 2020.1.25 | 8:21:15.00 | 38.22154 | 38.80174 | $13.00^l$ | $m_b$ 3.8 | 80 | 0.98 | 1.34 | 4.1 |
| 2020.1.25 | 8:40:3.18 | 38.48738 | 39.29502 | $13.00^n$ | $m_b$ 4.1 | 82 | 0.74 | 1.00 | 2.3 |
| 2020.1.25 | 10:14:56.40 | 38.27789 | 38.78064 | $9.00^l$ | $m_b$ 4.3 | 73 | 0.75 | 1.03 | 2.4 |
| 2020.1.25 | 16:30:8.38 | 38.38449 | 39.12238 | $10.00^n$ | $m_b$ 4.5 | 87 | 0.77 | 1.14 | 2.8 |
| 2020.1.25 | 16:44:1.09 | 38.40671 | 39.15789 | $8.00^n$ | $m_b$ 4.0 | 82 | 0.77 | 0.98 | 2.4 |
| 2020.1.25 | 16:46:57.89 | 38.42312 | 39.10487 | $7.00^n$ | $m_b$ 4.2 | 275 | 1.27 | 1.68 | 6.7 |
| 2020.1.26 | 2:22:46.25 | 38.25544 | 38.80843 | $13.00^l$ | $m_b$ 4.2 | 77 | 0.76 | 1.04 | 2.5 |
| 2020.1.27 | 16:11:59.75 | 38.39131 | 39.14291 | $8.00^n$ | $m_b$ 3.8 | 79 | 0.72 | 0.92 | 2.1 |
| 2020.1.31 | 15:36:12.26 | 38.45117 | 39.17154 | $10.00^n$ | $m_b$ 3.8 | 74 | 1.24 | 1.67 | 6.5 |
| 2020.1.31 | 23:32:49.18 | 38.48315 | 39.32654 | $15.00^n$ | $m_b$ 4.3 | 81 | 0.73 | 0.93 | 2.1 |
| 2020.2.1 | 0:3:49.36 | 38.41196 | 39.30329 | $10.00^l$ | $m_b$ 3.9 | 271 | 0.85 | 1.16 | 3.1 |
| 2020.2.3 | 22:19:40.64 | 38.39001 | 39.13978 | $9.00^n$ | $m_b$ 4.0 | 87 | 0.88 | 1.16 | 3.2 |
| 2020.2.4 | 3:40:44.56 | 38.37960 | 39.14839 | $9.00^n$ | $-$ 3.5 | 283 | 1.09 | 1.66 | 5.7 |
| 2020.2.7 | 19:57:4.98 | 38.44685 | 39.23547 | $12.00^n$ | $-$ 3.8 | 81 | 1.40 | 1.65 | 7.3 |
| 2020.2.10 | 22:4:10.30 | 38.32459 | 38.90359 | $15.00^n$ | $-$ 3.9 | 73 | 1.42 | 1.93 | 8.6 |
| 2020.2.12 | 9:35:16.48 | 38.46626 | 39.25430 | $14.00^n$ | $-$ 3.8 | 82 | 1.15 | 1.48 | 5.3 |
| 2020.2.13 | 17:28:45.56 | 38.46715 | 39.33021 | $11.00^l$ | $-$ 3.5 | 81 | 1.33 | 1.80 | 7.5 |
| 2020.2.16 | 16:40:32.56 | 38.30579 | 38.74588 | $16.00^l$ | $-$ 3.7 | 274 | 1.07 | 1.39 | 4.7 |
| 2020.2.17 | 11:42:13.24 | 38.35697 | 39.14049 | $10.00^l$ | $-$ 4.4 | 78 | 1.25 | 2.01 | 7.9 |
| 2020.2.20 | 0:13:55.04 | 38.28922 | 38.75579 | $16.00^l$ | $-$ 3.8 | 71 | 1.11 | 1.40 | 4.9 |

**Table S4.**    Calibrated hypocenters of the Samandag cluster, where direct calibration was achieved with data from epicentral distances of $<1.0°$ and the 90% hypocentroid uncertainty is 0.7 km. Columns are as in Table S2.

| Date | Time | Lat | Lon | Depth | Mag | A1 | L1 | L2 | Area |
|------|------|-----|-----|-------|-----|-----|-----|-----|------|
| 1988.8.3 | 20:42:30.78 | 36.01273 | 35.81363 | $14.00^d$ | $m_b$ 4.6 | 340 | 0.92 | 1.32 | 3.8 |
| 1989.6.24 | 3:9:56.24 | 36.79035 | 36.05383 | $20.00^d$ | $m_b$ 5.0 | 285 | 1.01 | 1.48 | 4.7 |
| 1996.1.21 | 9:28:40.28 | 35.96644 | 35.64992 | $14.00^l$ | – | 338 | 0.65 | 1.42 | 2.9 |
| 1996.6.4 | 17:42:46.16 | 35.79456 | 35.75190 | $19.00^d$ | $m_b$ 4.0 | 333 | 1.20 | 1.91 | 7.2 |
| 1996.6.18 | 23:44:12.34 | 36.08579 | 36.06778 | $14.00^l$ | $m_b$ 4.1 | 347 | 1.21 | 1.25 | 4.8 |
| 1996.6.19 | 0:18:3.42 | 36.05863 | 36.08459 | $14.00^l$ | $m_b$ 4.4 | 346 | 0.76 | 1.05 | 2.5 |
| 1997.1.22 | 17:57:20.08 | 36.26675 | 36.07198 | $13.70^m$ | $m_b$ 5.4 | 335 | 0.71 | 0.86 | 1.9 |
| 1997.1.22 | 18:24:51.77 | 36.24250 | 36.01614 | $15.00^m$ | $m_b$ 5.1 | 335 | 0.75 | 0.88 | 2.1 |
| 1997.1.22 | 18:27:30.29 | 36.29300 | 36.10557 | $7.00^l$ | $m_b$ 5.2 | 322 | 0.85 | 1.00 | 2.7 |
| 1997.1.23 | 7:9:23.55 | 36.32203 | 36.17902 | $13.90^m$ | $m_b$ 4.3 | 359 | 0.84 | 1.14 | 3.0 |
| 2002.3.11 | 1:19:34.71 | 36.77597 | 36.06846 | $12.30^m$ | $m_b$ 3.9 | 348 | 1.44 | 1.48 | 6.7 |
| 2003.1.3 | 6:49:24.70 | 36.05343 | 35.86090 | $12.00^l$ | $m_b$ 4.2 | 33 | 1.07 | 1.57 | 5.3 |
| 2003.2.26 | 3:8:20.95 | 35.84666 | 36.36828 | $12.90^m$ | $m_b$ 4.4 | 358 | 0.78 | 1.11 | 2.7 |
| 2006.2.21 | 0:40:24.53 | 36.08667 | 35.91884 | $16.30^m$ | – | 345 | 0.71 | 0.97 | 2.2 |
| 2006.3.29 | 22:5:13.38 | 35.34386 | 35.48569 | $17.00^l$ | $m_b$ 4.7 | 360 | 0.83 | 0.98 | 2.5 |
| 2006.9.19 | 0:28:53.54 | 36.08155 | 35.75060 | $16.00^l$ | $m_b$ 4.0 | 6 | 0.98 | 1.52 | 4.7 |
| 2006.10.9 | 5:1:33.49 | 35.87461 | 35.56771 | $14.00^l$ | $m_b$ 4.5 | 345 | 0.70 | 0.90 | 2.0 |
| 2007.2.1 | 23:4:16.85 | 35.97343 | 35.87987 | $16.40^m$ | $m_b$ 4.2 | 22 | 0.85 | 1.05 | 2.8 |
| 2007.3.11 | 20:11:49.06 | 36.51694 | 35.88883 | $12.00^l$ | $m_b$ 3.7 | 329 | 1.02 | 1.12 | 3.6 |
| 2007.5.12 | 13:6:41.23 | 36.41167 | 35.67977 | $11.00^l$ | – | 14 | 0.90 | 1.29 | 3.6 |
| 2007.6.13 | 21:54:36.66 | 35.98679 | 35.76380 | $13.00^n$ | $M_D$ 3.6 | 5 | 0.77 | 1.10 | 2.7 |
| 2008.5.3 | 3:20:53.39 | 36.62390 | 36.64098 | $14.00^l$ | $m_b$ 3.7 | 7 | 1.02 | 1.39 | 4.5 |
| 2008.6.19 | 0:24:33.02 | 36.65174 | 36.00630 | $7.00^l$ | – | 78 | 1.14 | 1.47 | 5.3 |
| 2009.1.22 | 4:43:5.46 | 36.09394 | 35.83537 | $20.00^n$ | $M_L$ 3.3 | 12 | 1.00 | 1.16 | 3.6 |
| 2009.4.16 | 12:57:4.57 | 36.11874 | 35.80078 | $19.00^n$ | – | 332 | 0.87 | 1.03 | 2.8 |
| 2009.6.17 | 4:29:14.30 | 36.14057 | 36.02046 | $17.30^m$ | $m_b$ 4.8 | 318 | 0.73 | 0.87 | 2.0 |
| 2009.10.27 | 20:54:49.04 | 36.29835 | 35.53812 | $14.00^l$ | $m_b$ 3.7 | 339 | 0.89 | 1.00 | 2.8 |
| 2010.3.7 | 23:28:55.11 | 36.57141 | 36.44286 | $12.00^l$ | $m_b$ 3.6 | 349 | 1.00 | 1.56 | 4.9 |
| 2010.11.14 | 23:8:26.59 | 36.60635 | 36.02914 | $12.00^l$ | $m_b$ 5.0 | 335 | 0.81 | 0.87 | 2.2 |
| 2011.3.17 | 18:54:25.34 | 35.72720 | 36.26244 | $18.10^m$ | $m_b$ 3.4 | 358 | 0.70 | 1.03 | 2.3 |
| 2011.6.28 | 9:29:18.62 | 36.02946 | 35.82704 | $15.40^m$ | $m_b$ 3.4 | 348 | 0.65 | 0.90 | 1.8 |
| 2013.7.26 | 0:22:56.40 | 36.06156 | 35.87515 | $17.00^n$ | $m_b$ 4.2 | 349 | 0.76 | 0.99 | 2.3 |
| 2013.8.6 | 14:54:47.30 | 36.38346 | 35.66598 | $11.00^l$ | $m_b$ 3.5 | 359 | 0.94 | 1.07 | 3.1 |
| 2014.2.14 | 0:33:38.22 | 36.74572 | 36.02443 | $12.00^l$ | $m_b$ 4.6 | 355 | 0.69 | 0.80 | 1.7 |
| 2014.6.9 | 3:38:36.13 | 36.75343 | 36.03594 | $17.00^l$ | $m_b$ 4.7 | 4 | 0.77 | 0.85 | 2.0 |
| 2014.7.12 | 21:58:22.96 | 36.59720 | 35.89924 | $11.00^l$ | $m_b$ 3.6 | 1 | 0.77 | 0.91 | 2.2 |
| 2014.9.3 | 3:15:30.03 | 36.61592 | 35.92335 | $12.00^l$ | – | 7 | 0.96 | 1.28 | 3.9 |
| 2015.2.10 | 4:1:55.79 | 36.08315 | 35.93577 | $10.00^l$ | $m_b$ 4.5 | 355 | 0.78 | 0.87 | 2.1 |
| 2015.3.25 | 2:17:0.66 | 36.29679 | 35.91520 | $7.00^l$ | – | 57 | 0.98 | 1.10 | 3.4 |
| 2015.9.6 | 15:35:54.80 | 36.74975 | 36.13088 | $10.00^l$ | – | 40 | 1.57 | 2.19 | 10.8 |

| Date | Time | Lat | Lon | Depth | Mag | A1 | L1 | L2 | Area |
|------|------|-----|-----|-------|-----|----|----|----|------|
| 2016.3.28 | 0:26:26.49 | 36.07370 | 35.74773 | $13.00^l$ | – | 3 | 0.73 | 0.99 | 2.3 |
| 2016.5.22 | 6:19:8.36 | 36.10417 | 36.38318 | $19.00^l$ | $m_b$ 3.6 | 40 | 0.91 | 1.28 | 3.7 |
| 2017.5.13 | 19:41:43.96 | 36.12366 | 35.65431 | $15.40^m$ | – | 358 | 0.75 | 0.90 | 2.1 |
| 2017.8.25 | 21:45:31.85 | 36.47158 | 35.92930 | $8.00^l$ | $M_L$ 2.7 | 9 | 1.06 | 1.47 | 4.9 |
| 2017.9.25 | 21:6:40.20 | 36.66326 | 35.95613 | $10.00^l$ | $M_w$ 3.2 | 322 | 0.94 | 1.15 | 3.4 |
| 2017.10.5 | 23:9:46.23 | 35.57265 | 36.42504 | $9.00^l$ | $M_D$ 3.1 | 1 | 0.85 | 1.66 | 4.4 |
| 2017.10.18 | 16:26:34.91 | 36.14275 | 35.87488 | $14.80^m$ | $M_L$ 3.1 | 357 | 0.96 | 1.14 | 3.4 |
| 2017.11.24 | 17:59:34.41 | 36.13618 | 35.84733 | $12.50^m$ | $M_L$ 3.3 | 8 | 0.86 | 1.05 | 2.8 |
| 2019.2.20 | 5:35:21.78 | 36.10355 | 35.92041 | $10.00^l$ | $m_b$ 4.2 | 3 | 0.84 | 1.00 | 2.6 |
| 2019.4.10 | 21:2:37.53 | 36.65751 | 36.14050 | $8.70^m$ | $M_w$ 3.8 | 61 | 0.93 | 1.12 | 3.3 |
| 2019.4.15 | 20:10:58.47 | 36.21526 | 36.03903 | $8.50^m$ | $M_L$ 3.0 | 74 | 0.99 | 1.75 | 5.4 |
| 2019.9.18 | 23:19:10.97 | 36.10247 | 35.87167 | $8.80^m$ | $M_l$ 3.3 | 45 | 0.99 | 1.28 | 4.0 |

**Table S5.** Calibrated hypocenters of the Golbasi cluster, where direct calibration was achieved with data from epicentral distances of $<0.7°$ and the 90% hypocentroid uncertainty is 0.6 km. Columns are as in Table S2.

| Date | Time | Lat | Lon | Depth | Mag | A1 | L1 | L2 | Area |
|------|------|-----|-----|-------|-----|----|----|----|------|
| 1986.5.5 | 3:35:37.90 | 37.98932 | 37.78351 | $5.00^d$ | $m_b$ 6.0 | 282 | 0.96 | 1.27 | 3.8 |
| 1986.6.6 | 10:39:47.88 | 38.00864 | 37.93164 | $18.00^d$ | $m_b$ 5.7 | 287 | 1.00 | 1.09 | 3.4 |
| 1986.6.6 | 11:29:44.95 | 38.04502 | 37.92342 | $5.00^d$ | $m_b$ 4.5 | 347 | 2.03 | 2.31 | 14.7 |
| 1986.8.3 | 1:33:22.22 | 37.08313 | 37.18752 | $26.00^d$ | $m_b$ 5.0 | 55 | 1.13 | 1.30 | 4.6 |
| 2000.4.2 | 11:41:25.23 | 37.68026 | 37.28079 | $8.00^l$ | $m_b$ 4.5 | 291 | 1.47 | 1.53 | 7.1 |
| 2000.4.2 | 17:26:53.11 | 37.68304 | 37.31483 | $10.00^l$ | $m_b$ 4.3 | 280 | 0.95 | 2.12 | 6.3 |
| 2002.11.19 | 1:25:35.49 | 38.04914 | 38.43176 | $5.00^l$ | $m_b$ 4.7 | 11 | 1.19 | 1.38 | 5.1 |
| 2003.4.2 | 20:55:41.06 | 38.03467 | 38.19649 | $12.00^l$ | $m_b$ 4.2 | 33 | 1.48 | 1.88 | 8.7 |
| 2004.2.26 | 4:13:57.59 | 37.98790 | 38.26793 | $9.00^l$ | $m_b$ 4.8 | 18 | 1.16 | 1.37 | 5.0 |
| 2006.3.15 | 21:6:43.39 | 37.45926 | 37.58948 | $13.00^n$ | – | 37 | 1.03 | 1.08 | 3.5 |
| 2006.4.23 | 4:0:28.12 | 37.49919 | 36.79792 | $14.00^l$ | $m_b$ 3.9 | 344 | 1.13 | 1.34 | 4.8 |
| 2006.7.20 | 18:7:50.84 | 38.05597 | 38.19887 | $12.00^l$ | $m_b$ 3.7 | 354 | 1.07 | 1.31 | 4.4 |
| 2006.7.24 | 23:4:58.34 | 37.52509 | 38.68066 | $14.00^l$ | $m_b$ 3.5 | 54 | 1.69 | 2.38 | 12.6 |
| 2007.8.24 | 2:53:11.24 | 38.14605 | 37.43726 | $12.00^l$ | $m_b$ 4.4 | 12 | 0.93 | 0.98 | 2.9 |
| 2007.9.15 | 5:26:52.37 | 37.86032 | 36.96848 | $8.00^l$ | $m_b$ 4.6 | 339 | 0.99 | 1.09 | 3.4 |
| 2007.9.15 | 23:28:48.19 | 37.84084 | 36.92079 | $10.00^l$ | $m_b$ 4.5 | 1 | 1.05 | 1.08 | 3.6 |
| 2008.8.20 | 11:1:38.55 | 37.69179 | 37.49732 | $9.00^l$ | $m_b$ 4.3 | 5 | 0.97 | 1.05 | 3.2 |
| 2008.9.3 | 2:22:47.07 | 37.48327 | 38.56939 | $10.00^l$ | $m_b$ 4.6 | 43 | 0.91 | 0.94 | 2.7 |
| 2008.9.3 | 2:25:16.53 | 37.51343 | 38.55459 | $6.00^l$ | $m_b$ 4.1 | 55 | 1.14 | 1.54 | 5.5 |
| 2008.9.4 | 22:54:32.34 | 37.47682 | 38.55766 | $11.00^l$ | $m_b$ 3.9 | 33 | 0.92 | 1.19 | 3.4 |
| 2009.2.26 | 8:53:42.39 | 37.19200 | 36.90282 | $11.00^l$ | $m_b$ 3.4 | 53 | 1.09 | 1.31 | 4.5 |
| 2012.4.4 | 11:5:16.97 | 36.95781 | 37.03857 | $16.00^n$ | $m_b$ 3.8 | 67 | 1.03 | 1.36 | 4.4 |
| 2012.5.25 | 11:22:39.77 | 38.13414 | 38.60756 | $9.00^l$ | $m_b$ 4.2 | 81 | 0.95 | 1.00 | 3.0 |
| 2012.9.8 | 10:1:6.84 | 37.32099 | 37.12768 | $10.00^l$ | $m_b$ 4.1 | 73 | 1.05 | 1.29 | 4.2 |
| 2012.9.19 | 9:17:46.68 | 37.30072 | 37.13169 | $13.00^n$ | $m_b$ 4.9 | 272 | 0.86 | 0.97 | 2.6 |
| 2012.9.19 | 23:15:7.42 | 37.32548 | 37.12673 | $12.00^n$ | $m_b$ 3.8 | 82 | 0.92 | 1.09 | 3.2 |
| 2012.9.20 | 1:10:29.12 | 37.32928 | 37.11732 | $15.00^n$ | – | 71 | 0.88 | 1.02 | 2.8 |
| 2012.10.16 | 1:16:3.06 | 37.31591 | 37.12471 | $14.00^n$ | $m_b$ 4.3 | 76 | 0.82 | 0.87 | 2.2 |
| 2012.10.16 | 10:25:4.88 | 37.30653 | 37.11135 | $14.00^n$ | $m_b$ 4.3 | 73 | 0.86 | 1.04 | 2.8 |
| 2012.11.13 | 23:55:49.26 | 37.28798 | 37.12888 | $18.00^n$ | $m_b$ 4.4 | 40 | 0.87 | 0.96 | 2.6 |
| 2012.11.14 | 0:1:59.65 | 37.31848 | 37.13173 | $15.00^n$ | $m_b$ 3.9 | 69 | 1.02 | 1.10 | 3.5 |
| 2012.12.1 | 3:51:43.34 | 37.51394 | 38.36549 | $12.00^n$ | – | 57 | 0.90 | 1.12 | 3.2 |
| 2012.12.24 | 4:14:49.17 | 37.85950 | 37.01200 | $10.00^l$ | $m_b$ 3.4 | 21 | 1.10 | 1.20 | 4.2 |
| 2013.1.8 | 6:5:8.10 | 37.90600 | 37.96125 | $13.00^l$ | $m_b$ 4.3 | 299 | 1.04 | 1.06 | 3.5 |
| 2013.1.8 | 6:15:5.24 | 37.90648 | 37.94233 | $12.00^l$ | $m_b$ 4.0 | 64 | 1.01 | 1.16 | 3.7 |
| 2013.2.12 | 20:20:32.77 | 37.06521 | 36.92031 | $9.00^l$ | – | 62 | 0.88 | 1.12 | 3.1 |
| 2013.4.19 | 20:50:0.63 | 37.33860 | 37.11111 | $12.00^n$ | – | 83 | 1.04 | 1.31 | 4.3 |
| 2013.4.21 | 21:6:30.68 | 37.31246 | 37.09399 | $12.00^n$ | – | 76 | 1.03 | 1.21 | 3.9 |
| 2013.4.25 | 22:54:15.94 | 37.31853 | 37.09367 | $14.00^n$ | $m_b$ 3.9 | 81 | 0.98 | 1.13 | 3.5 |

| Date | Time | Lat | Lon | Depth | Mag | A1 | L1 | L2 | Area |
|---|---|---|---|---|---|---|---|---|---|
| 2013.5.1 | 6:47:56.94 | 37.28458 | 37.10344 | $14.00^n$ | – | 272 | 1.09 | 1.45 | 4.9 |
| 2013.5.1 | 6:50:52.69 | 37.30573 | 37.09095 | $12.00^n$ | $m_b$ 3.7 | 87 | 1.07 | 1.41 | 4.8 |
| 2013.5.6 | 18:33:18.87 | 37.33070 | 37.11301 | $14.00^n$ | $m_b$ 3.4 | 64 | 0.94 | 1.08 | 3.2 |
| 2013.6.16 | 20:31:39.09 | 38.10703 | 37.06639 | $10.00^l$ | $m_b$ 3.8 | 19 | 1.03 | 1.20 | 3.9 |
| 2014.3.26 | 14:0:15.06 | 38.14534 | 38.58401 | $11.00^l$ | $m_b$ 3.9 | 77 | 1.07 | 1.14 | 3.8 |
| 2014.8.28 | 10:22:1.13 | 37.11339 | 36.88937 | $13.00^n$ | $m_b$ 3.7 | 60 | 0.90 | 1.14 | 3.2 |
| 2015.2.12 | 18:52:6.29 | 38.14888 | 38.46498 | $13.00^n$ | – | 61 | 1.03 | 1.14 | 3.7 |
| 2015.8.26 | 23:1:44.45 | 37.31076 | 36.97412 | $12.00^n$ | $m_b$ 4.1 | 67 | 0.87 | 1.02 | 2.8 |
| 2016.9.16 | 5:12:24.15 | 37.19936 | 36.91429 | $13.00^n$ | – | 34 | 0.93 | 1.09 | 3.2 |
| 2017.3.2 | 11:7:25.29 | 37.61073 | 38.45165 | $15.00^n$ | $m_b$ 5.3 | 58 | 0.76 | 0.81 | 1.9 |
| 2017.3.2 | 11:18:17.91 | 37.55655 | 38.41864 | $14.00^n$ | $m_b$ 3.7 | 64 | 1.14 | 1.34 | 4.8 |
| 2017.3.2 | 17:3:2.35 | 37.58842 | 38.48276 | $12.00^n$ | $m_b$ 3.3 | 47 | 1.01 | 1.19 | 3.8 |
| 2017.3.2 | 23:10:53.23 | 37.61431 | 38.46678 | $12.00^n$ | – | 68 | 0.89 | 1.05 | 2.9 |
| 2017.3.3 | 20:51:53.93 | 37.61413 | 38.45484 | $14.00^n$ | – | 77 | 0.87 | 1.07 | 2.9 |
| 2017.3.10 | 22:23:42.65 | 37.58668 | 38.49432 | $13.00^n$ | $m_b$ 3.4 | 72 | 0.90 | 1.04 | 2.9 |
| 2017.3.28 | 21:53:30.78 | 38.31295 | 37.18004 | $16.00^n$ | $m_b$ 3.8 | 342 | 0.96 | 1.07 | 3.2 |
| 2017.8.18 | 4:30:1.24 | 37.57420 | 37.56508 | $14.00^n$ | $M_w$ 4.3 | 51 | 0.84 | 0.94 | 2.5 |
| 2017.8.30 | 7:34:3.97 | 37.67175 | 37.44404 | $12.00^n$ | $M_L$ 3.9 | 66 | 0.85 | 1.15 | 3.1 |
| 2017.12.8 | 4:31:50.24 | 37.25792 | 37.15866 | $11.00^n$ | $M_L$ 3.9 | 80 | 0.89 | 1.00 | 2.8 |
| 2017.12.16 | 8:39:25.18 | 37.39108 | 37.67031 | $10.00^n$ | $M_w$ 3.9 | 44 | 0.96 | 1.04 | 3.1 |
| 2018.4.24 | 0:34:29.23 | 37.60104 | 38.49900 | $13.00^n$ | $m_b$ 5.1 | 72 | 0.74 | 0.79 | 1.8 |
| 2018.5.21 | 1:9:24.45 | 37.47304 | 38.59109 | $13.00^n$ | $M_w$ 4.0 | 79 | 0.86 | 1.16 | 3.1 |
| 2018.7.3 | 13:16:18.41 | 37.69151 | 37.41398 | $12.00^n$ | $M_w$ 4.1 | 61 | 0.80 | 0.88 | 2.2 |
| 2018.10.2 | 15:29:3.96 | 37.68636 | 37.42844 | $13.00^n$ | $M_w$ 4.4 | 65 | 0.82 | 0.90 | 2.3 |
| 2019.3.22 | 10:4:7.52 | 37.22493 | 36.89973 | $7.00^n$ | $M_w$ 3.9 | 65 | 0.82 | 0.98 | 2.5 |
| 2019.7.19 | 16:47:7.01 | 37.69257 | 37.43257 | $14.00^n$ | $M_w$ 3.7 | 70 | 0.97 | 1.17 | 3.6 |

March 25, 2020, 9:12pm

:

**Table S6.** Calibrated hypocenters of the Bingöl cluster, where direct calibration was achieved with data from epicentral distances of $<0.8°$ and the 90% hypocentroid uncertainty is 0.8 km. Columns are as in Table S2.

| Date | Time | Lat | Lon | Depth | Mag | A1 | L1 | L2 | Area |
|------|------|-----|-----|-------|-----|----|----|----|------|
| 1971.5.22 | 16:43:57.52 | 38.93962 | 40.51021 | $6.00^d$ | $M_S$ 6.9 | 278 | 1.31 | 1.53 | 6.3 |
| 1975.9.6 | 9:20:7.25 | 38.54419 | 40.67216 | $12.00^d$ | $M_S$ 6.6 | 89 | 1.16 | 1.36 | 4.9 |
| 1975.9.6 | 12:10:41.98 | 38.39910 | 40.47928 | $9.00^d$ | $m_b$ 4.9 | 89 | 1.55 | 2.22 | 10.8 |
| 1976.9.5 | 22:7:31.14 | 38.49562 | 40.84386 | $11.00^d$ | $m_b$ 5.0 | 275 | 1.62 | 2.23 | 11.3 |
| 1976.10.8 | 17:11:52.82 | 38.60067 | 40.41345 | $19.00^d$ | $m_b$ 4.9 | 61 | 2.12 | 2.86 | 19.0 |
| 1977.3.25 | 2:39:55.12 | 38.68835 | 39.92097 | $13.00^d$ | $m_b$ 5.1 | 85 | 1.62 | 2.22 | 11.3 |
| 1980.7.11 | 12:33:25.98 | 38.55451 | 40.77618 | $17.00^d$ | $m_b$ 5.1 | 90 | 1.42 | 1.96 | 8.7 |
| 1992.5.7 | 19:15:2.12 | 38.80201 | 40.01878 | $18.00^d$ | $m_b$ 5.1 | 282 | 1.40 | 1.78 | 7.8 |
| 1996.12.20 | 8:9:1.65 | 39.18563 | 40.72440 | $14.00^d$ | $m_b$ 4.2 | 297 | 1.37 | 3.56 | 15.3 |
| 1998.10.8 | 20:48:6.86 | 38.89481 | 40.28956 | $12.00^l$ | $m_b$ 4.5 | 5 | 1.96 | 2.60 | 16.0 |
| 2003.5.1 | 0:27:3.22 | 39.08154 | 40.44389 | $12.00^d$ | $M_S$ 6.3 | 37 | 1.05 | 1.06 | 3.5 |
| 2003.5.1 | 9:35:51.49 | 38.98219 | 40.58995 | $11.00^n$ | $m_b$ 4.1 | 79 | 2.57 | 3.85 | 31.1 |
| 2003.5.4 | 2:9:56.82 | 39.08540 | 40.49387 | $10.00^n$ | $m_b$ 4.3 | 55 | 1.77 | 1.90 | 10.6 |
| 2003.5.21 | 3:11:15.27 | 38.75037 | 40.59104 | $14.00^n$ | $m_b$ 3.8 | 277 | 1.85 | 2.41 | 14.0 |
| 2007.1.26 | 8:20:34.46 | 38.77978 | 40.10091 | $8.00^l$ | $m_b$ 4.5 | 24 | 1.48 | 1.71 | 7.9 |
| 2007.1.26 | 11:43:33.22 | 38.83077 | 40.05399 | $12.00^l$ | $m_b$ 3.2 | 323 | 1.86 | 2.07 | 12.1 |
| 2008.6.21 | 3:58:34.34 | 38.97620 | 41.28443 | $14.00^l$ | $m_b$ 4.2 | 19 | 1.10 | 1.41 | 4.9 |
| 2008.6.21 | 4:46:32.91 | 38.98080 | 41.32839 | $12.00^l$ | $m_b$ 3.7 | 11 | 1.09 | 1.90 | 6.5 |
| 2008.6.29 | 15:37:3.32 | 38.97614 | 41.30603 | $12.00^n$ | $m_b$ 3.9 | 23 | 1.10 | 1.46 | 5.0 |
| 2009.8.26 | 4:32:25.27 | 39.03726 | 41.15123 | $14.00^n$ | $m_b$ 3.2 | 7 | 1.24 | 2.17 | 8.4 |
| 2010.2.14 | 12:20:49.63 | 38.75657 | 40.04345 | $12.00^l$ | $m_b$ 3.4 | 45 | 1.06 | 1.34 | 4.5 |
| 2010.2.21 | 4:38:35.32 | 38.73555 | 40.06970 | $11.00^l$ | $m_b$ 3.8 | 46 | 0.94 | 1.02 | 3.0 |
| 2010.3.8 | 2:32:31.04 | 38.83697 | 40.02717 | $14.00^l$ | $M_S$ 6.0 | 45 | 0.93 | 0.95 | 2.8 |
| 2010.3.8 | 3:20:23.87 | 38.84035 | 40.15332 | $12.00^l$ | $m_b$ 4.1 | 34 | 1.09 | 1.15 | 3.9 |
| 2010.3.8 | 7:47:39.07 | 38.78813 | 40.11412 | $15.00^l$ | $m_b$ 5.4 | 27 | 0.91 | 0.94 | 2.7 |
| 2010.3.8 | 8:11:20.54 | 38.77118 | 40.04064 | $10.00^l$ | $m_b$ 4.1 | 9 | 1.03 | 1.14 | 3.7 |
| 2010.3.8 | 9:0:46.21 | 38.78691 | 40.07495 | $10.00^l$ | $m_b$ 4.6 | 8 | 1.03 | 1.08 | 3.5 |
| 2010.3.8 | 9:21:58.59 | 38.82661 | 40.06855 | $11.00^l$ | – | 329 | 1.26 | 1.44 | 5.7 |
| 2010.3.8 | 9:30:4.95 | 38.87087 | 40.16225 | $12.00^l$ | – | 40 | 1.00 | 1.10 | 3.4 |
| 2010.3.8 | 10:14:23.96 | 38.86424 | 40.10456 | $14.00^l$ | $m_b$ 5.0 | 66 | 1.09 | 1.19 | 4.1 |
| 2010.3.8 | 11:12:10.74 | 38.80621 | 40.09495 | $13.00^l$ | $m_b$ 4.9 | 30 | 0.91 | 0.95 | 2.7 |
| 2010.3.8 | 14:17:34.31 | 38.78376 | 40.06067 | $10.00^l$ | $m_b$ 3.6 | 357 | 1.05 | 1.25 | 4.1 |
| 2010.3.8 | 15:4:51.77 | 38.78498 | 40.06470 | $14.00^l$ | $m_b$ 4.6 | 24 | 1.09 | 1.21 | 4.1 |
| 2010.3.9 | 0:9:18.59 | 38.77554 | 40.05228 | $11.00^l$ | $m_b$ 3.4 | 19 | 1.06 | 1.09 | 3.6 |
| 2010.3.9 | 6:14:56.91 | 38.76364 | 40.09925 | $11.00^l$ | $m_b$ 3.6 | 44 | 1.02 | 1.24 | 4.0 |
| 2010.3.9 | 7:21:23.69 | 38.89482 | 40.23252 | $13.00^l$ | $m_b$ 4.0 | 42 | 1.03 | 1.20 | 3.9 |
| 2010.3.9 | 7:34:34.99 | 38.79661 | 40.08387 | $12.00^l$ | $m_b$ 3.4 | 45 | 1.05 | 1.21 | 4.0 |
| 2010.3.12 | 1:35:13.00 | 38.74453 | 40.08988 | $12.00^l$ | – | 44 | 1.03 | 1.07 | 3.5 |
| 2010.3.12 | 22:50:44.34 | 38.82347 | 40.06416 | $12.00^l$ | $m_b$ 3.5 | 55 | 0.98 | 1.09 | 3.4 |
| 2010.3.24 | 14:11:29.85 | 38.81683 | 40.16385 | $8.00^l$ | $m_b$ 5.0 | 35 | 0.99 | 1.11 | 3.5 |

| Date | Time | Lat | Lon | Depth | Mag | A1 | L1 | L2 | Area |
|---|---|---|---|---|---|---|---|---|---|
| 2010.4.24 | 5:15:7.10 | 38.82724 | 40.12414 | $15.00^l$ | $m_b$ 3.4 | 62 | 1.00 | 1.33 | 4.2 |
| 2010.6.27 | 13:27:36.67 | 38.34116 | 41.04385 | $16.00^n$ | $m_b$ 3.4 | 6 | 1.11 | 1.21 | 4.2 |
| 2012.4.28 | 3:17:4.36 | 38.53160 | 40.74913 | $12.00^l$ | $m_b$ 4.7 | 52 | 0.98 | 0.99 | 3.1 |
| 2014.3.16 | 2:38:58.27 | 38.57863 | 40.69187 | $13.00^l$ | $m_b$ 3.5 | 35 | 0.89 | 1.10 | 3.1 |
| 2014.9.28 | 8:22:15.83 | 38.85917 | 40.97451 | $16.00^n$ | $m_b$ 3.2 | 83 | 0.96 | 1.10 | 3.3 |
| 2015.5.9 | 21:35:3.19 | 38.67266 | 40.14641 | $13.00^l$ | $m_b$ 3.5 | 20 | 0.99 | 1.27 | 4.0 |
| 2015.6.13 | 1:3:15.37 | 38.65541 | 40.18620 | $12.00^l$ | $m_b$ 3.4 | 14 | 0.95 | 1.10 | 3.3 |
| 2016.6.10 | 18:57:0.80 | 39.02460 | 40.73201 | $15.00^n$ | $m_b$ 4.0 | 341 | 1.02 | 1.09 | 3.5 |
| 2017.3.20 | 4:36:57.41 | 38.71800 | 40.14928 | $12.00^l$ | – | 38 | 0.94 | 1.01 | 3.0 |
| 2018.3.24 | 15:4:5.72 | 38.33175 | 40.96489 | $14.00^n$ | $M_w$ 4.1 | 6 | 0.97 | 1.01 | 3.1 |
| 2019.8.10 | 20:16:0.76 | 38.91492 | 40.07125 | $17.00^l$ | $M_w$ 3.6 | 331 | 1.46 | 1.59 | 7.3 |
| 2019.8.12 | 13:34:26.41 | 38.33995 | 40.85899 | $13.00^l$ | $m_b$ 4.1 | 300 | 1.14 | 1.31 | 4.7 |

**Table S7.**  Uniform slip inversion results using one fault. Northings and Eastings in km are

the projected center of the surface break (UTM 37N).

| Parameters | Fault n.1 |
|---|---|
| *Strike* | 243.2 |
| *Dip* | 76.2 |
| *Rake* | 0.3 |
| *Slip (m)* | 0.85 |
| *Eastings (km)* | 502.994 |
| *Northings (km)* | 4 241.546 |
| *Length (km)* | 36.5 |
| *Top depth (km)* | 1.3 |
| *Bottom depth (km)* | 21.3 |

**Table S8.** Uniform slip inversion results using two faults. For the first pair of fault, we fixed the strike, length and position (Lon, Lat) according to the EAF mapping (Duman & Emre, 2013). The dip, rake and depths (top and bottom) were left as free parameters. Northings and Eastings in km are the projected center of the surface break (UTM 37N). To reduce the number of free parameters we fixed the fault slip at one meter.

| Parameters | Fault n.1 | Fault n.2 | Fault n.1 | Fault n.2 |
|---|---|---|---|---|
| *Strike* | 245 | 233 | 244.7 | 243.1 |
| *Dip* | 80.4 | 61.9 | 80.0 | 64.0 |
| *Rake* | 1.9 | -6.01 | 2.7 | -18.3 |
| *Slip* ($m$) | 1 | 1 | 1 | 1 |
| *Eastings* ($km$) | 507.959 | 493.460 | 505.6617 | 494.300 |
| *Northings* ($km$) | 4 245.704 | 4 237.142 | 4 243.1364 | 4 235.270 |
| *Length* ($km$) | 24 | 12 | 22.3 | 15.0 |
| *Topdepth* ($km$) | 2.1 | 1.2 | 1.5 | 3.0 |
| *Bottomdepth* ($km$) | 19.1 | 14.8 | 16.6 | 14.5 |
| Source | (Duman & Emre, 2013) and uniform inversion | | Uniform inversion | |

**Table S9.**   Other published source parameters for the 2020 Elazığ mainshock. GCMT =
Global Centroid Moment Tensor project; USGS = United States Geological Survey ANSS Com-
prehensive Earthquake Catalog (ComCat); Mww = $W$-phase moment tensor; Mwr = regional
moment tensor; Mwb = body wave tensor. Lon. and lat. refer to the longitude and latitude of
the GCMT centroid and the USGS epicenter; depth refers to the centroid depth.

| Source | Lon. | Lat. | Strike | Dip | Rake | Depth | Seismic moment | $M_w$ |
|---|---|---|---|---|---|---|---|---|
| GCMT | 39.00° | 38.30° | 246° | 67° | −9° | 12 km | $1.77 \times 10^{19}$ Nm | 6.8 |
| USGS Mww | 39.088° | 38.390° | 245° | 80° | −12° | 22 km | $1.39 \times 10^{19}$ Nm | 6.7 |
| USGS Mwr | 39.088° | 38.390° | 246° | 77° | 0° | 11 km | $0.60 \times 10^{19}$ Nm | 6.5 |
| USGS Mwb | 39.088° | 38.390° | 250° | 85° | 1° | 16 km | $1.23 \times 10^{19}$ Nm | 6.7 |

**Table S10.**    Aftershock focal mechanisms from regional waveform modeling. Epicenters given to four decimal places are from our own relocations; those given to two decimal places are from the European-Mediterranean Seismological Centre. CD is the centroid depth in kilometers.

| Date | Time (UTC) | Lat. (°N) | Lon. (°E) | CD | $M_w$ | Strike (°) | Dip (°) | Rake (°) |
|------|-----------|-----------|-----------|-----|-------|-----------|---------|----------|
| 2020.1.25 | 00:57:17.65 | 38.3562 | 39.0942 | 4 | 3.9 | 248 | 70 | 8 |
| 2020.1.25 | 06:07:33.00 | 38.3468 | 39.0772 | 4 | 4.1 | 243 | 58 | -14 |
| 2020.1.25 | 08:40:03.18 | 38.4873 | 39.2950 | 20 | 4.3 | 146 | 78 | -159 |
| 2020.1.25 | 16:30:08.38 | 38.3844 | 39.1223 | 3 | 4.9 | 153 | 71 | -159 |
| 2020.1.26 | 02:22:46.25 | 38.2554 | 38.8084 | 3 | 4.5 | 58 | 62 | -11 |
| 2020.1.27 | 16:11:59.75 | 38.3913 | 39.1429 | 3 | 4.3 | 71 | 63 | 0 |
| 2020.1.28 | 09:31:30.7 | 38.36 | 39.13 | 4 | 3.8 | 157 | 88 | -172 |
| 2020.1.29 | 02:11:53.46 | 38.43 | 39.30 | 2 | 3.9 | 334 | 76 | -167 |
| 2020.1.31 | 23:32:49.18 | 38.4831 | 39.3265 | 7 | 4.6 | 312 | 56 | -148 |
| 2020.2.1 | 00:03:49.36 | 38.4196 | 39.3032 | 2 | 4.1 | 246 | 87 | -3 |
| 2020.2.3 | 22:19:41.20 | 38.3900 | 39.1397 | 4 | 4.5 | 336 | 89 | 165 |
| 2020.2.4 | 20:37:13.0 | 38.35 | 39.07 | 4 | 3.7 | 243 | 66 | -7 |
| 2020.2.7 | 19:57:04.98 | 38.4468 | 39.2355 | 3 | 3.8 | 64 | 65 | -2 |
| 2020.2.12 | 09:35:16.48 | 38.4663 | 39.2543 | 7 | 3.8 | 320 | 88 | 176 |
| 2020.2.17 | 12:04:04 | 38.3570 | 39.1405 | 4 | 4.3 | 156 | 82 | -169 |

**Table S11.** More details about the aftershock regional waveform models. DC is the double couple component in %, VR is variance reduction, CN is the condition number, FMVAR is the focal mechanism variability index, STVAR is the space time variability index, # is the number of stations used, and filter is the frequency band used (E. N. Sokos & Zahradník, 2008; E. Sokos & Zahradník, 2013).

| Date | Time (UTC) | $M_0$ (Nm) | DC (%) | VR | CN | FMVAR | STVAR | # | Filter (Hz) |
|---|---|---|---|---|---|---|---|---|---|
| 2020.1.25 | 00:57:17.65 | $9.641 \times 10^{14}$ | 87.8 | 0.54 | 2.5 | 11±11 | 0.17 | 16 | 0.04–0.08 |
| 2020.1.25 | 06:07:33.00 | $1.665 \times 10^{15}$ | 42.0 | 0.53 | 2.5 | 20±9 | 0.28 | 16 | 0.04–0.08 |
| 2020.1.25 | 08:40:03.18 | $3.828 \times 10^{14}$ | 88.8 | 0.56 | 2.5 | 8±6 | 0.24 | 12 | 0.04–0.09 |
| 2020.1.25 | 16:30:08.38 | $3.144 \times 10^{16}$ | 71.0 | 0.60 | 4.5 | 12±6 | 0.23 | 9 | 0.02–0.08 |
| 2020.1.26 | 02:22:46.25 | $6.028 \times 10^{15}$ | 47.4 | 0.59 | 3.5 | 17±7 | 0.22 | 10 | 0.04–0.07 |
| 2020.1.27 | 16:11:59.75 | $3.792 \times 10^{15}$ | 65.3 | 0.70 | 2.6 | 12±8 | 0.14 | 12 | 0.04–0.09 |
| 2020.1.28 | 09:31:30.7 | $6.729 \times 10^{14}$ | 56.1 | 0.66 | 2.4 | 7±5 | 0.20 | 11 | 0.04–0.09 |
| 2020.1.29 | 02:11:53.46 | $8.529 \times 10^{14}$ | 62.4 | 0.58 | 3.8 | 8±5 | 0.12 | 13 | 0.04–0.09 |
| 2020.1.31 | 23:32:49.18 | $8.429 \times 10^{15}$ | 79.9 | 0.62 | 1.7 | 17±12 | 0.27 | 10 | 0.04–0.09 |
| 2020.2.1 | 00:03:49.36 | $2.022 \times 10^{15}$ | 53.2 | 0.63 | 4.5 | 8±5 | 0.27 | 7 | 0.04–0.09 |
| 2020.2.3 | 22:19:41.20 | $7.034 \times 10^{15}$ | 66.2 | 0.79 | 2.3 | 8±9 | 0.17 | 7 | 0.02–0.07 |
| 2020.2.4 | 20:37:13.0 | $4.817 \times 10^{14}$ | 54.3 | 0.53 | 2.4 | 14±7 | 0.19 | 8 | 0.05–0.09 |
| 2020.2.7 | 19:57:04.98 | $7.367 \times 10^{14}$ | 65.7 | 0.62 | 3.2 | 17±10 | 0.14 | 6 | 0.05–0.08 |
| 2020.2.12 | 09:35:16.48 | $5.710 \times 10^{14}$ | 96.8 | 0.63 | 1.6 | 2±1 | 0.25 | 6 | 0.04–0.09 |
| 2020.2.17 | 12:04:04 | $3.686 \times 10^{16}$ | 62.8 | 0.64 | 2.3 | 7±5 | 0.16 | 15 | 0.04–0.09 |